Energy 323 (2025) 135825

Contents lists available at ScienceDirect

Energy

journal homepage: www.elsevier.com/locate/energy

A comparative study of radiant floor heating strategies for passive house in severely cold regions: A case study of Harbin

Xiaoni Gao [a,b], Yuchen Ji [c], Pengyuan Shen [a,*]

[a] Institute of Future Human Habitats, Shenzhen International Graduate School, Tsinghua University, Shenzhen, China
[b] School of Architecture, Harbin Institute of Technology, Shenzhen, China
[c] College of Mechatronics and Control Engineering, Shenzhen University, Shenzhen, 518052, China

ARTICLE INFO

Handling editor: X Zhao

Keywords:
Passive house
Radiant floor
Energy use
Building heating
Building simulation
COMSOL

ABSTRACT

This study explores the efficient heating strategy for passive houses in severely cold climates to improve the indoor thermal environment. Intermittent heating strategies based on indoor temperature to radiant floor heating system are applied and various heating methods under three heating strategies for passive houses are simulated. We proposed three metrics to rate the effectiveness of heating strategies: the indoor comfort rate (ICR), the physical comfort rate (PCR), and the thermal response coefficient (TRC), which are integrated to evaluate the performance of heating strategies comprehensively. It is shown that outdoor temperature fluctuation has little influence on the choice of heating strategy for passive houses. Furthermore, the short-interval heating strategy's ICR and PCR are above 90 %, and the TRC is above 0.2 h^{-1}, demonstrating better performance than the continuous low temperature and long interval heating strategies. The results suggest the adoption of a short-interval heating mode for passive houses, with a suggested inlet water temperature of 60 °C and an indoor temperature control range of 22–26 °C. The study compares and analyzes three control strategies (continuous low-temperature heating, long interval heating, and short-interval heating), providing a reference for selecting appropriate heating strategies under different usage scenarios.

Nomenclature

ICR	Indoor comfort rate
PCR	Physical comfort rate
TCR	Thermal response coefficient
CFD	Computational fluid dynamics
PMV-PPD	Predicted Mean Vote - Predicted Percentage of Dissatisfied
EPS	Expanded Polystyrene Board
COMSOL	COMSOL Multiphysics
NMBE	Normalized Mean Bias Error
CV (RMSE)	Coefficient of Variation of Root Mean Square Error
R2	R-squared or Coefficient of Determination
δ	Thickness, m
ρ	Density, kg/m3
λ	Thermal Conductivity, W/m·K
C_p	Specific Heat Capacity, J/kg·K
U	U-value, W/(m2·K)
h_r	Radiation heat transfer coefficient, W/(m^2 •K)
ε	Surface emissivity of the ground
σ	Stefan-Boltzmann constant

(continued on next column)

(*continued*)

$T_{s,1}$	Surface temperature of the ground, K
T_{fj}	Area-weighted average temperature of the indoor non-heated surfaces, K
A_i	Surface area of the ith envelope structure in the sample room, m2
q_r	Radiation heat flux density, W/m^2
Nu	Nusselt number
C	Experimentally determined constant
Gr	Grashof number
Pr	Prandtl number
n	Experimentally determined constant
h_c	Surface heat transfer coefficient, W/(m2·K)
l	Characteristic dimension, m
q_c	Convection heat flux density, W/m2
T_a	Indoor air temperature, K
T_{total}	Total monitoring time, h
Vt	Volume
Dt	Diameter of the floor heating pipe
Subscripts	
in	Indoor

* Corresponding author. Shenzhen International Graduate School, Tsinghua University, 518055, China.
E-mail address: pengyuan_pub@163.com (P. Shen).

https://doi.org/10.1016/j.energy.2025.135825
Received 28 October 2024; Received in revised form 28 February 2025; Accepted 24 March 2025
Available online 26 March 2025
0360-5442/

1. Introduction

1.1. Background

With the rapid development of the global economy, energy consumption levels have steadily increased, with residential buildings accounting for approximately 35 % of total energy use. This proportion is expected to rise significantly in the coming years [1]. In cold regions, attention has shifted toward passive houses to meet the heating demands of residential buildings while reducing energy consumption [2–4]. Studies have shown that the energy consumption of passive houses is only one-tenth that of conventional residential buildings [5,6]. Additionally, research indicates that if passive houses and similar ultra-low-energy buildings expand to one-third of the global building stock by 2050, this could help limit the global temperature rise to within 1.5 °C by 2050 [7,8].

Despite their widespread popularity worldwide [9], passive houses often fail to meet the indoor comfort demands of residents in cold regions due to their extreme climate conditions. Studies indicate that passive houses often present issues related to discomfort despite their energy-saving features [10,11]. For example, a previous study conducted a survey and interviews on the satisfaction of residents living in passive houses, revealing that 48 % of the homes did not meet the WHO's recommended indoor temperature [12]. Liu et al. investigated whether passive houses in cold regions satisfy human thermal comfort requirements and found that these buildings often suffer from inadequate heating, necessitating additional heating systems to raise indoor temperatures [13]. Zhang et al. employed statistical methods to observe and analyze temperature fluctuations in a passive house in a cold region. Their results showed that significant heat loss occurred at night, requiring 315.51 kg of fuel to maintain an appropriate indoor temperature [14]. Moreover, comparative studies [15–17] demonstrated that improving the airtightness and insulation of passive houses could reduce electricity consumption by 20.76 % during the entire heating season. However, cold regions still require supplementary heating systems to achieve thermal comfort indoors during the winter.

1.2. Literature review

Previous studies have extensively explored radiant floor heating systems to improve the indoor thermal environment of passive houses in cold regions, providing residents with a more comfortable living experience. Research on radiant floor heating systems indicates that they ensure indoor air distribution that meets human thermal comfort requirements [14,18] while also offering advantages such as energy efficiency [19,20] and space-saving benefits [20–22]. Additionally, experimental studies show that residents using radiant floor heating systems report a satisfaction rate of up to 71 % with the comfort of indoor spaces compared to other heating systems [23]. Recent research has changed the focus from continuous high-temperature operation to intermittent high-temperature heating (long breaks, short heating periods, relying on the building's thermal inertia to maintain indoor temperatures) [24–28] and continuous low-temperature operation [29–32]. The goal is to improve the temperature and thermal conditions inside passive houses in cold areas while using less heating energy. For instance, Benakopoulos et al. tested and simulated the energy and cost savings of these two heating strategies, finding that both ensured indoor thermal comfort and achieved approximately 11 % energy savings in specific buildings [33]. However, the study did not analyze the advantages and disadvantages of intermittent high-temperature and continuous low-temperature strategies or examine the appropriate scenarios for applying these heating methods.

Moreover, heating control strategies based on indoor air temperature or thermal comfort (short-intervals, with frequent on-off cycles based on indoor temperature) have significantly improved indoor comfort [22,34]. However, due to poor airtightness in existing buildings, short-interval heating strategies tend to cause frequent cycling, leading to high energy consumption. Consequently, air conditioning systems commonly apply this method [25,35,36], but no studies have yet explored its application in radiant floor heating systems. For instance, Zhang et al. [37] proposed a method for dynamically controlling indoor air temperature through air conditioning systems using the HRE (Heat Recovery Efficiency) index, which is based on exhaust air temperature, supply air temperature, and indoor air temperature. The PMV (Predicted Mean Vote) equation determines the desired indoor air temperature to achieve optimal thermal comfort. This method helps update supply conditions to meet the required thermal comfort levels. Similarly, Zampetti et al. [38] used PMV measurements taken from various subzones as control variables to regulate the air conditioning system, achieving energy savings of up to 17 % compared to traditional on-off control systems. Fang et al. [39] investigated the performance of ground-source heat pumps in maintaining indoor environments, establishing a relationship between heat pump power and indoor PMV values to identify optimal performance for balancing low energy consumption and suitable thermal comfort. Mao et al. [40–42] proposed a method to reduce the energy consumption of bedroom TAC (Temperature and Airflow Control) systems while keeping PMV values at thermally neutral levels. Given that passive houses are highly airtight compared to traditional buildings, applying short-interval heating control strategies to the radiant floor heating systems in passive houses could significantly enhance thermal comfort in indoor spaces.

There are many methods available to evaluate the thermal comfort of heating strategies, such as PMV-PPD calculation analysis [43–47], indoor temperature field [36,48,49], and CFD comfort simulation analysis [50–52] with consideration of asymmetric thermal radiation impact [53]. However, these methods evaluate heating outcomes mainly based on static environmental control scenario, without considering the practical implications in dynamic control applications. Furthermore, intermittent heating strategies involve multiple on-and-off cycles, leading to significant fluctuations in indoor temperature. Evaluating indoor thermal comfort solely based on temperature changes may not comprehensively assess the thermal environment [54,55]. In fact, when evaluating heating strategies for residential buildings, it is essential to consider not only temperature variation and energy consumption but also factors such as occupant satisfaction with thermal comfort [56], actual human thermal comfort [57], and system response time [58,59], all of which offer significant practical value. This is particularly relevant because intermittent heating strategies have the following characteristics: 1) unpredictable timing of changes [29], 2) uncertain amplitude of temperature fluctuations [60], and 3) unpredictable frequency of intermittence [61]. Therefore, analyzing heating strategies from an engineering application perspective can provide valuable insights into water supply temperature and operational timing, as well as improve energy management efficiency.

As previously mentioned, numerous researchers have studied the control methods of passive houses and radiant floor heating systems. First, while passive houses have become a key focus in developing energy-efficient buildings, relying solely on passive design in cold regions often fails to meet indoor comfort requirements. On the other hand, continuous heating using traditional methods leads to significant energy waste. Second, control strategies based on indoor air temperature have been shown to improve thermal comfort significantly, but their application to radiant floor heating systems still needs to be explored. Third, comparative studies on the three control strategies for radiant floor heating systems—continuous low-temperature heating, long-interval heating, and short-interval heating—are still lacking. Lastly, there is a lack of comprehensive methods for evaluating heating strategies from the perspective of engineering applications.

1.3. Objectives of the study

In this study, to achieve an optimal heating strategy, enhance energy efficiency, and improve indoor thermal comfort in cold regions, a comparative experiment was conducted. This paper introduces a radiant floor heating model based on passive houses in cold regions. It simulates the performance of three control strategies under varying outdoor temperatures in these cold climates. Based on the simulation results, a comparative analysis of the three control strategies for floor radiant heating systems in passive houses is conducted, providing useful insights for future heating mode selection. Therefore, the novelty of this study lies in three key aspects.

(1) This study explores an efficient heating strategy for passive houses to improve their indoor thermal environment.
(2) It provides a reference for selecting the appropriate heating strategy under different usage scenarios.
(3) From an engineering application perspective, three evaluation criteria for heating strategies are proposed.

This paper begins with on-site measurements of the radiant floor heating system in passive houses located in severely cold regions. Based

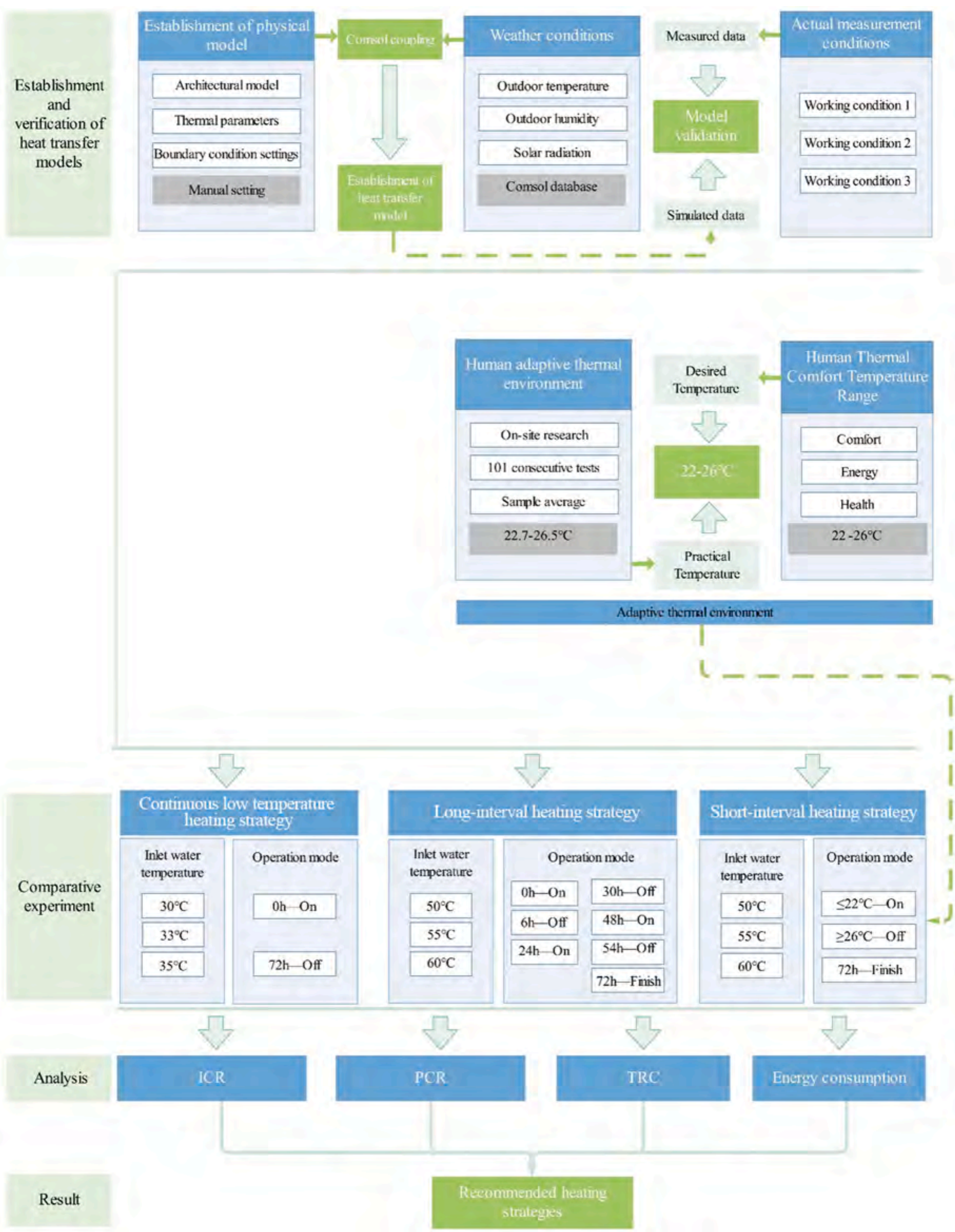

Fig. 1. Comparative study flow.

on the measurement results, a numerical model was developed to simulate the operational modes of three heating strategies. Subsequently, from an engineering application perspective, the numerical model was used to evaluate the energy consumption, occupant satisfaction with thermal comfort, actual human thermal comfort, and system response time for each heating strategy. Finally, based on the evaluation results, an efficient heating strategy suitable for passive houses in extreme climate conditions is proposed to improve their indoor thermal environment and provide a reference for selecting an appropriate heating strategy in different usage scenarios.

2. Methodology

To facilitate an understanding of the research methodology, Fig. 1 outlines the process of the comparative study on heating strategies for passive houses. First, a passive house model is established using COMSOL Multiphysics, with simulations conducted based on the software's heat transfer in solids and non-isothermal pipe flow modules. Next, the validated heat transfer model simulates three different heating strategies: continuous low-temperature heating, long-interval heating, and short-interval heating. The simulation results are then evaluated in terms of indoor comfort rate (ICR), personal comfort rate (PCR), thermal response coefficient (TRC), and energy consumption. Finally, based on the analysis, recommendations are provided for the appropriate application scenarios for the three heating strategies.

2.1. Establishment of heat transfer model

2.1.1. Building simulation model

Harbin, located in the north-east of China, is a typical city in the country's severe cold regions. Its winters (from December to February) are extremely cold, with average temperatures typically ranging from −16 °C to −22 °C. The lowest historical temperature recorded in the coldest month (usually January) has reached an astonishing −38.1 °C, according to meteorological data, making Harbin one of the coldest cities in China during the winter. Furthermore, during extreme cold weather, Harbin is often struck by "cold waves," a drastic temperature drop caused by the rapid southward movement of cold air from the north. When a cold wave strikes, daytime temperatures can drop by more than 10 °C, accompanied by strong north winds that further intensify the sensation of cold. These climatic conditions necessitate buildings to have excellent insulation properties and place higher demands on energy consumption, particularly in terms of heating. Therefore, this study is about a passive residential building located in Harbin (Fig. 2). The building has three floors with two rows of 24 rooms (Fig. 3 (a)). The primary heat sources for this building are a high-efficiency air-source heat pump and a solar thermal system, which are supplemented by an energy storage system and an auxiliary heating system (electric heating) to meet heating demands during extreme weather conditions. Under normal heating conditions, the building typically relies on the air-source heat pump and solar thermal system to provide energy, storing any excess energy. However, in extreme climate conditions, when the efficiency of the air-source heat pump and solar thermal system is reduced due to external environmental factors and

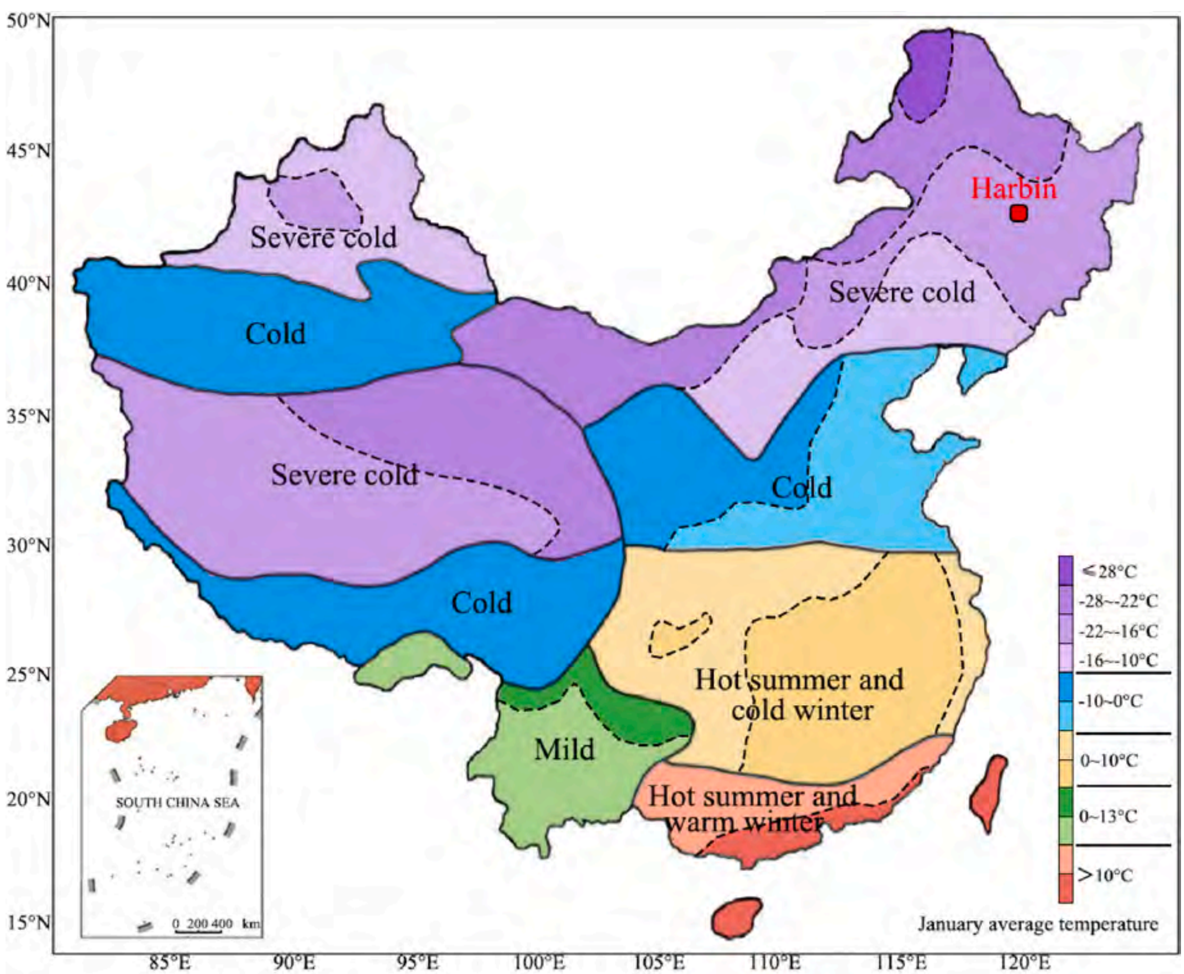

Fig. 2. Climate zones of China.

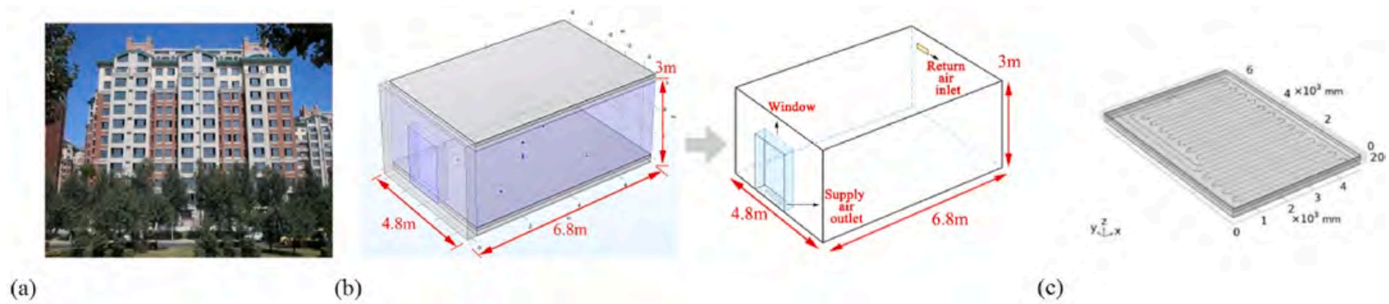

Fig. 3. Simulation Object:(a) Passive house façade, (b) Simplified Model, (c) Floor geometry model.

they can only provide limited heat, the heating system activates the energy storage device or auxiliary heating unit to supplement the heat supply. These performance parameters comply with the German Passive House Standards. The building also features a centralized ventilation system that operates year-round to meet residents' needs for fresh air.

For this study, one unit of the building was selected for the simulation, and a simplified model was developed (Fig. 3 (a)). The simulated unit measures 6.8 m in length, 4.8 m in width, and 3 m in height Fig. 3 (b). Fig. 3 (c) depicts the floor geometry model. The heating pipes are made of PB material, laid in a serpentine pattern, with an inner diameter of 0.016m, an outer diameter of 0.020m, and a spacing of 0.250m between pipes. The distance from the floor's bottom surface to the center of the pipes is 0.070m. The structural and design parameters for the simulation are listed in Table 1.

2.1.2. Boundary condition settings

To accurately simulate the indoor temperature field, set the following boundary conditions after establishing the model.

(1) Determine the boundary conditions for the water pipe's inlet and outlet. The inlet boundary condition for the water pipes is defined as a velocity boundary, with the inlet water flow velocity set at 0.3 m/s based on experimentally measured parameters. A thermal outflow serves as the outlet boundary.
(2) Define the interface between the pipes and the ceiling: The pipe walls are heat transfer surfaces, with a thermal conductivity of 0.12 W/m·K and a wall thickness of 0.002m. Additionally, an internal thermal resistance is applied. The heat transfer equation is expressed as Eq. (1) [26]:

Table 1
Parameter settings.

Physical quantity	Parameter Value
Wooden floor	$\delta = 0.010$m, $\lambda = 0.173$ W/m·K, $\rho = 700$ kg/m^3, $C_p = 2310$ J/kg·K
Foam padding	$\delta = 0.003$m, $\lambda = 0.047$ W/m·K, $\rho = 100$ kg/m^3, $C_p = 1380$ J/kg·K
Blockboard	$\delta = 0.012$m, $\lambda = 0.017$ W/m·K, $\rho = 600$ kg/m^3, $C_p = 2510$ J/kg·K
Leveling layer	$\delta = 0.015$m, $\lambda = 0.093$ W/m·K, $\rho = 1800$ kg/m^3, $C_p = 1050$ J/kg·K
Reinforced concrete floor	$\delta = 0.160$m, $\lambda = 1.74$ W/m·K, $\rho = 250000$ kg/m^3, $C_p = 920$ J/kg·K
Internal plastering	$\delta = 0.020$m, $\lambda = 0.93$ W/m·K, $\rho = 1800$ kg/m^3, $C_p = 1050$ J/kg·K
Exterior wall (brick, EPS)	$\delta = 0.670$m, U = 0.13 W/(m^2·K)
Windows (triple-layer Low-E glass)	$\delta = 0.044$m, U = 0.8 W/(m^2·K)
Door	$\delta = 0.080$m, U = 1 W/(m^2·K)
fluid	Selected from COMSOL material library
Tube spacing	0.250m
Water flow rate	0.3 m/s
Buried pipe depth	0.070m
Heating indoor temperature	22 °C

$$Nu_{\text{int}} = \frac{(f_D/8)(R_e - 1000)P_r}{1 + 12.7(f_D/8)^{1/2}\left(P_r^{2/3} - 1\right)} \tag{1}$$

where,

$$\Pr = \frac{C_p\mu}{k}$$

$$h_{\text{int}} = Nu_{\text{int}}\frac{k}{d_h}$$

(3) Define the ceiling boundary: The upper and lower surfaces are set with radiation and convection heat transfer boundaries, respectively, and the other surfaces are set as thermal insulation, that is, Eq. (2):

$$-n \cdot q = 0 \tag{2}$$

2.1.3. Model validation

This study validates the simulation platform through a series of experiments. The operating conditions of the selected simulation target were measured from January 1 to January 18, 2018, and the same conditions were simulated using the software. The simulated temperature values at corresponding measurement points in the model were then extracted and compared with the actual test results to verify the accuracy of the simulation method used in this study. To assess the model's performance, this study uses the following validation metrics: calibration criteria (NMBE, CV(RMSE) and R^2) [62–64], and S-M deviation (range, IQR, and median) [65,66]. Fig. 4 illustrates the model validation process, while Fig. 5 shows the measurement process and corresponding data. Table 2 presents the three experimental conditions.

The critical test parameters included the floor surface temperature, indoor air temperature, supply and return water temperatures, and the surface temperatures of other building envelope components. Five measurement points were placed on both the ceiling and the floor. In comparison, three points were evenly distributed along the horizontal centerline of the inner wall, outer wall, and inner surface of the exterior windows. Thermocouples were also positioned at 0.1 m, 0.6 m, 1.7 m, and 2.2 m above the ground to measure the indoor temperature. Fig. 6 displays the arrangement of the measurement points.

(1) Supply and return water temperatures: These were measured using a temperature and humidity recorder, with the measurement points located on the pipe walls at the thermal inlet of the experimental room.
(2) Surface temperatures of building envelope components and indoor temperature: The measurements were taken using copper-constantan thermocouples with the instrument model Agilent 34970.
(3) Experimental data were collected to calculate the radiation heat transfer coefficient, surface heat transfer coefficient, radiation

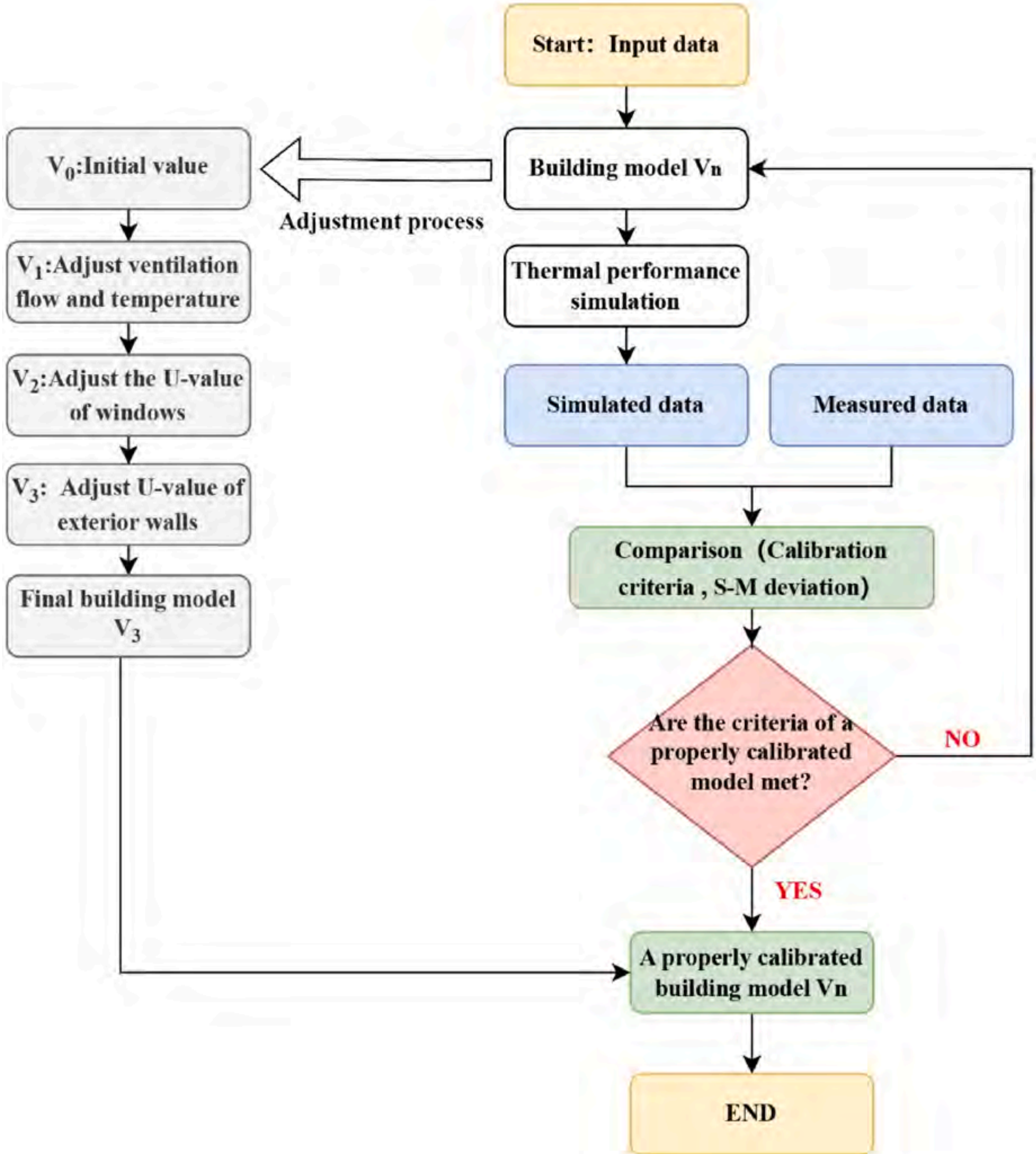

Fig. 4. The building model calibration process.

and convection heat flux densities, as well as the total heat flux density. Radiation heat transfer:

The radiation heat transfer coefficient for the ground is as follows, as shown in Eqs. (3) and (4).

$$h_r = \varepsilon\sigma \frac{T_{s,1}^4 - T_{fj}^4}{T_{s,1} - T_{fj}} \tag{3}$$

$$T_{fj} = \frac{A_i T_{s,i}}{\sum_{i=2}^{7} A_i} \tag{4}$$

h_r is the radiation heat transfer coefficient, W/(m^2 •K); ε is the surface emissivity of the ground, which is taken as 0.9; σ is the Stefan-Boltzmann constant, with a value of 5.67 × 10^{-8}W/(m^2 •K^4); $T_{s,1}$ represents the surface temperature of the ground, K; T_{fj} is the area-weighted average temperature of the indoor non-heated surfaces, K; non-heated surfaces include the ceiling, south exterior wall, south exterior window, east wall, west wall, and the inner surface of the north wall. A_i is the surface area of the i-th envelope structure in the sample room, m^2.

The formula for calculating radiation heat flux density is as follows, as shown in Eq. (5).

$$q_r = h_r (T_s - T_{fj}) \tag{5}$$

Where q_r is the radiation heat flux density, W/m^2.

Convection heat transfer: The surface heat transfer coefficient and convection heat flux density in this test are calculated based on the empirical correlations for natural convection heat transfer, as shown in Eqs. (6) and (7).

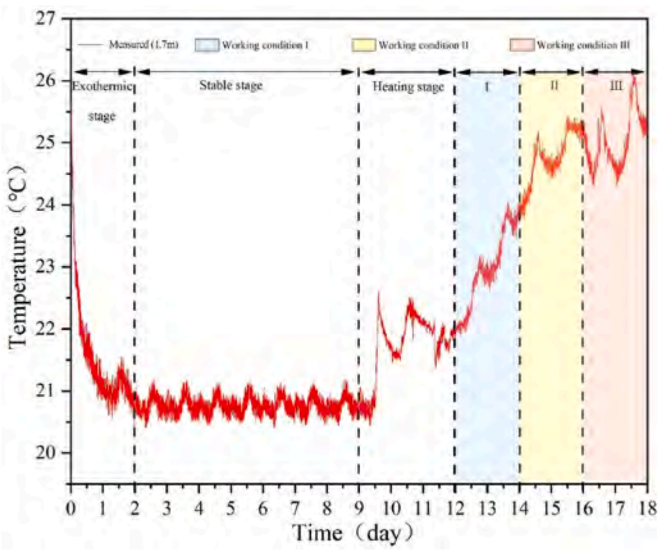

Fig. 5. Measured data from January 1 to January 18, 2018:The first 2 days (0–2) represent the transition of the passive house from the initial heating phase to the heat release stage. Days 2–9 correspond to the steady state after the heat release is completed. From days 9–12, the heating phase is set with an inlet water temperature of 30 °C and a flow rate of 0.22 m^3/h. Days 12–14 correspond to Condition 1, while days 14–16 correspond to Condition 2, and days 16–18 correspond to Condition 3. The parameter settings for Conditions 1, 2, and 3 are shown in Table 2.

Table 2
Test conditions.

Working conditions	Date	Water temperature	Flow
1	January 12–14	30 °C	0.22 m^3/h
2	January 14–16	31 °C	0.36 m^3/h
3	January 16–18	32 °C	0.36 m^3/h

$$\mathrm{Nu} = C(Gr \cdot Pr)^n \tag{6}$$

Where Nu is the Nusselt number; C is an experimentally determined constant, with a value of 0.54; Gr is the Grashof number; Pr is the Prandtl number; n is an experimentally determined constant, with a value of 0.25.

$$h_c = \frac{Nu \cdot \lambda}{l} \tag{7}$$

Where h_c is the surface heat transfer coefficient, W/(m^2·K); λ is the thermal conductivity, W/(m·K); l is the characteristic dimension, taken as the average length and width of the envelope surface, m.

The formula for calculating the convection heat flux density is as follows, as shown in Eq. (8).

$$q_c = h_c\left(T_{s,1} - T_a\right) \tag{8}$$

Where q_c is the convection heat flux density, W/m^2; T_a is the indoor air temperature, K。

The daily average radiation heat flux densities for operating conditions 1–3 were 15.38 W/m^2, 20.59 W/m^2, and 22.68 W/m^2, respectively, while the daily average convection heat flux densities were 1.42 W/m^2, 1.89 W/m^2, and 2.13 W/m^2, respectively. A comparison reveals that radiation heat transfer contributes approximately 91.5 % to the total heat flux density, which is one order of magnitude higher than convection heat transfer. In calculating the ground radiation heat transfer, the total heat flux density can be estimated based on the radiation heat flux density. Both the radiation heat transfer coefficient and the surface heat transfer coefficient increase with the supply water temperature.

Finally, the simulation model V_3 demonstrated excellent performance in terms of calibration criteria and S-M deviation for all measured variables, meeting the expected calibration standards and fulfilling engineering accuracy requirements (Figs. 7 and 8 and Table 3). Regarding calibration indicators, the NMBE was −0.94 % for both hourly and daily intervals. The CV(RMSE) was 1.13 % (hourly) and 1.15 % (daily). Additionally, the coefficient of determination (R^2) reached 0.90. For the S-M deviation parameters, the Range was 1.29, the IQR was 0.31 °C, and the Median was −0.23 °C. These results indicate that the model's predicted values closely align with the observed values, with the data distribution being compact and the central tendency nearly zero. This suggests that the model excels at temperature prediction under varying conditions. Overall, the results indicate that simulation model V_3 can accurately reflect the operational characteristics of the actual system, making it suitable for replacing real systems in studies of passive house operation and control.

2.2. External conditions

2.2.1. Necessity of outdoor temperature control

In this study, when conducting the radiant floor heat transfer simulation using COMSOL Multiphysics, it was decided after discussion and analysis to use stable outdoor temperature data for the simulation. In this study, both long-interval and short-interval heating strategies necessitate transient simulations. Considering outdoor temperature

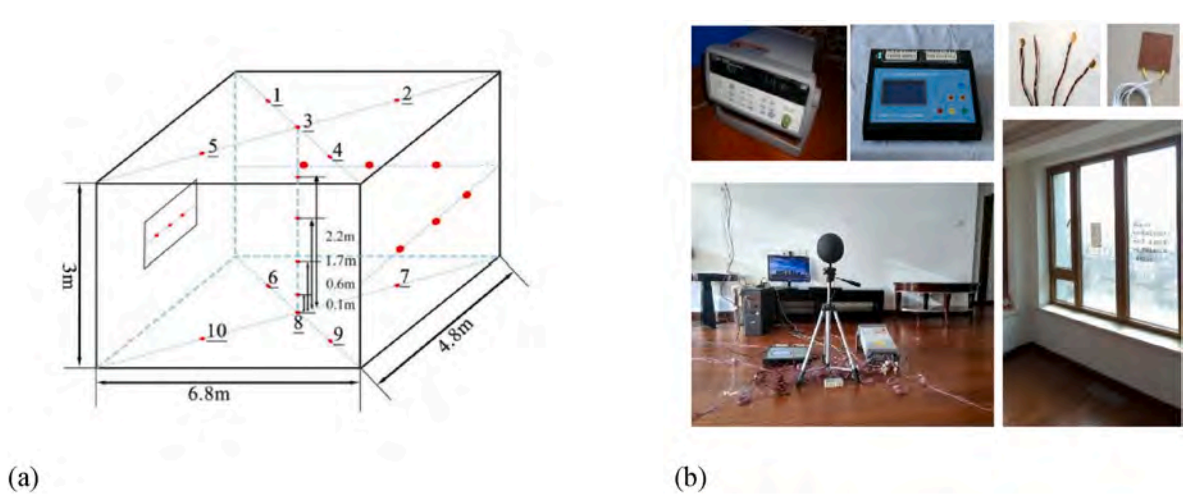

Fig. 6. (a) Measurement point layout, (b) Test equipment and field test photos.

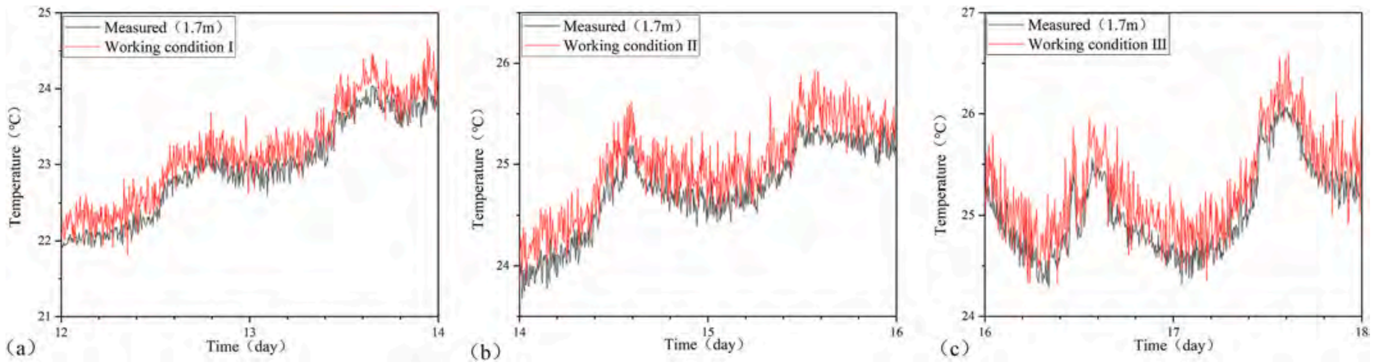

Fig. 7. Measured and simulated temperature values of the 1.7m height during the monitoring period.

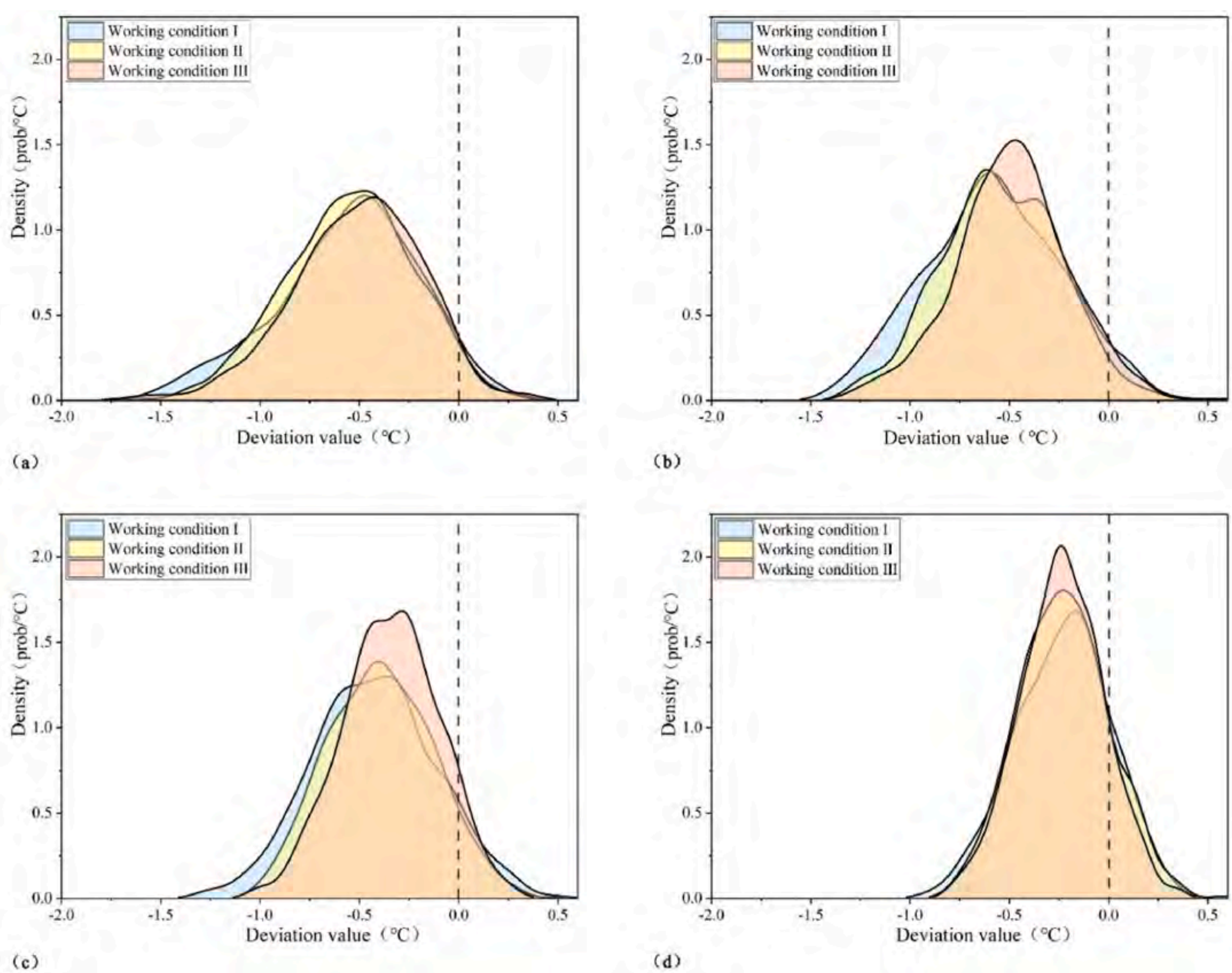

Fig. 8. The floor surface temperature calibration, shown as Simulation-Measurement (S–M) deviation histograms: (a) building model V_0; (b) building model V_1; (c) building model V_2; (d) building model V_3.

variations over time in transient simulations would significantly increase the complexity of the model [67,68]. If the model becomes overly complex, it may lead to increased computational difficulty or even result in the inability to obtain meaningful outcomes. Therefore, in the early assessment phase, fixed outdoor temperatures were chosen to conserve computational resources. To eliminate the complex impact of fluctuating outdoor temperatures on the indoor thermal environment and make the heat transfer model easier to analyze and understand [69–73]. Additionally, to focus the study on comparing the control strategies of indoor radiant floor heating systems, fixed outdoor temperature was selected.

Table 3
Averaged values of statistical calibration indicators (NMBE, CVRMSE and R^2) and S-M deviations (range, IQR, and median) for all measured temperature variables in the final calibrated model (V_3).

Statistical indicators		Calculation intervals	
Calibration criteria	NMBE	Hourly intervals	−0.94 %
		Daily intervals	−0.94 %
	CV(RMSE)	Hourly intervals	1.13 %
		Daily intervals	1.15 %
	R^2	Total measurement time	0.90
S-M deviation	Range (°C)		1.29
	IQR (°C)		0.31
	Median (°C)		−0.23

2.2.2. Outdoor air temperature setting

Harbin, as one of the representative cities in cold regions, experiences extremely low winter temperatures, particularly in January, when the average minimum temperature can reach −22 °C [72,74]. Meteorological data and historical temperature records indicate that many winter days in Harbin see temperatures below −20 °C, with extreme weather occasionally bringing prolonged periods of outdoor temperatures as low as −30 °C [75,76].

The study of heating strategies for passive houses is only meaningful under such low outdoor temperature conditions [77,78]. Due to their excellent insulation and energy efficiency, passive houses generally require little to no active heating during typical cold seasons [79,80]. Designed with auxiliary heating systems, passive houses primarily aim to manage extreme weather conditions to maintain indoor comfort in all situations [5,81,82].

To determine the appropriate outdoor temperature setting for the passive house used in this study, a heat dissipation simulation was conducted under normal indoor temperature conditions (Fig. 9). The results show that when the outdoor temperature is below −20 °C, the cooling rate of the passive house, initially at 22 °C, increases significantly. Therefore, to ensure indoor comfort in the passive house, activate the auxiliary heating system when the outdoor temperature drops below −20 °C.

Lower outdoor temperatures are advantageous for comparing heating systems under different control strategies [11]. When other conditions are the same, the lower the outdoor temperature, the more obvious the comparison of research results from different heating control strategies [34,83–86]. According to statistics, Table 4 presents the commonly used outdoor temperature reference values from existing studies.

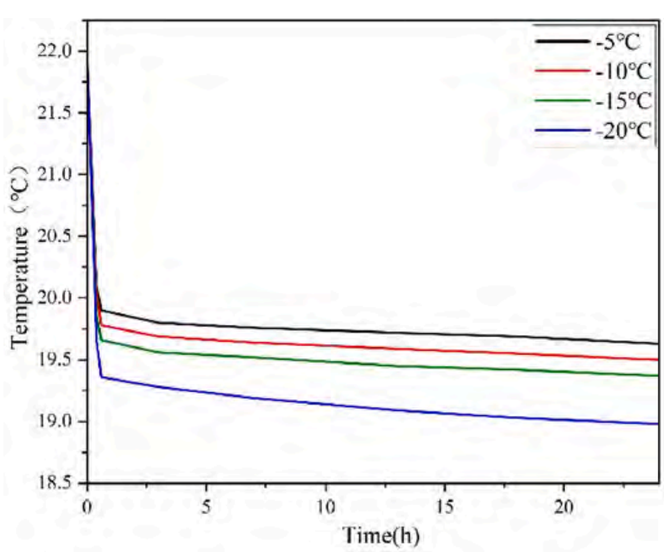

Fig. 9. Automatic heat release time of passive houses at different outdoor temperatures.

In summary, to reduce the simulation duration while evaluating the impact of outdoor temperatures on passive house heating modes in cold regions, this study ultimately selected outdoor temperatures of −20 °C, −25 °C, and −30 °C for the simulations.

2.3. Adaptive thermal environment

Table 5 and Fig. 10present the statistical results of the indoor environmental parameters for passive houses in Harbin during winter. This study conducted on-site investigations of the indoor thermal environment and thermal comfort in different households within passive residential buildings in Harbin. The indoor air temperature during winter was found to range primarily between 22.7 °C and 26.5 °C, with an average indoor air temperature of 25.5 °C and an average relative humidity of 31.3 %.

People generally prefer indoor temperatures to range from 22 °C to 26 °C, as this is considered optimal for both comfort and energy efficiency [87,88]. From a health perspective, this temperature range is also associated with reduced susceptibility to illness [89]. Consequently, setting the indoor temperature between 22 °C and 26 °C better aligns with individuals' thermal expectations and practical usage needs compared to the 18 °C–22 °C range.

2.4. Typical heating patterns of passive houses

Passive house heating strategies generally include continuous and intermittent operation modes. Intermittent operation can be further divided into two categories: the long-interval heating strategy, which is based on energy consumption, and the short-interval heating strategy, which employs a start-stop control pattern regulated by indoor temperature.

2.4.1. Continuous low temperature heating

A continuous low-temperature heating strategy aims to maintain comfortable indoor temperatures through sustained, low-intensity heating while optimizing energy efficiency. The simulation of this strategy set the inlet water temperature of the heating system at 30 °C, 33 °C, and 35 °C, with a flow rate of 0.3 m/s. The heating system was activated at hour 0 and deactivated after 72 h.

2.4.2. Long-interval heating

In the long-interval heating strategy, the heating system operates at longer intervals rather than continuously, briefly activating to maintain indoor temperatures within a comfortable range [81]. In the simulation of this strategy, the inlet water temperature was set at higher values of 50 °C, 55 °C, and 60 °C, with a flow rate of 0.3 m/s. The heating system was turned on for 6 h and then off for 18 h. Fig. 11 and Table 6 provide the on-off control schedule for the long-interval heating strategy.

2.4.3. Short-interval heating

The short-interval heating system operates based on real-time fluctuations in indoor air temperature to maintain the temperature within the specified comfort range. In the simulation of this strategy, the inlet water temperature was set to higher values of 50 °C, 55 °C, and 60 °C, with a flow rate of 0.3 m/s. The comfort range was set between 22 °C

Table 4
Commonly used outdoor temperature benchmarks.

Temperature	Applicable regions
0 °C	Cold winter areas
10 °C	Mild temperatures, spring or fall transition season
−5 °C	Colder winters in temperate regions
−20 °C	Cold regions
−30 °C	Extremely cold regions or low temperature environments

Table 5
Winter indoor environmental parameters of passive housing in Harbin.

Environmental parameters	Mean	Maximum	Minimum	Standard Deviation	Sample size
Air temperature (°C)	25.5	26.5	22.7	1.58	Continuous testing
Relative humidity (%)	31.3	46.1	18.4	8.62	101
Air velocity (m/s)	0.05	0.15	0.03	0.03	
Black globe temperature (°C)	26.1	28.8	22.9	1.30	
Operating temperature (°C)	26.2	27.7	22.8	1.27	

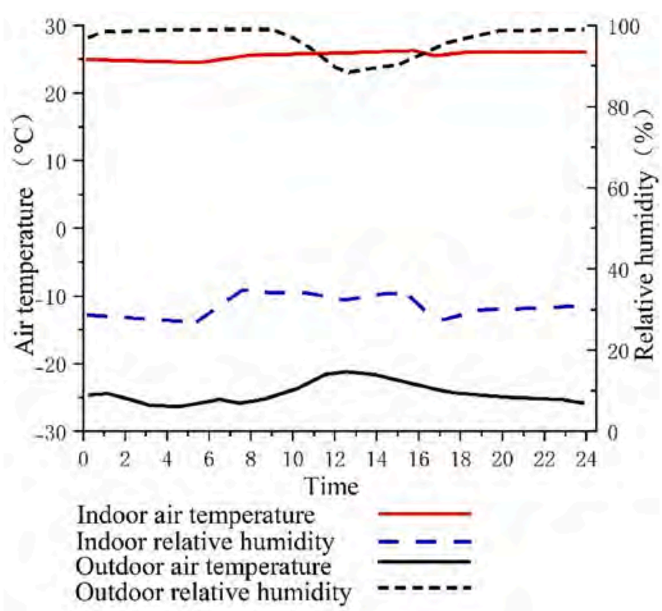

Fig. 10. Indoor and outdoor air temperature and relative humidity on January 15, 2016.

and 26 °C, with the heating system activating when the indoor temperature dropped below 22 °C and deactivating as it approached 26 °C.

2.5. Evaluation indicators

To accurately evaluate the heating performance of different strategies, this study introduced three additional evaluation metrics alongside energy consumption. The comparison of heating strategies was conducted from three perspectives: indoor thermal comfort satisfaction, actual human thermal comfort, and system response time. The following section provides an overview of these four evaluation criteria.

2.5.1. The indoor comfort rate (ICR)

Fig. 12 illustrates the significant fluctuations in indoor temperature, particularly during intermittent heating. Thus, evaluating the performance of heating strategies requires calculating the ratio of the total effective time that the indoor temperature remains within the thermal comfort zone to the overall heating duration. To quantify the effectiveness of different heating strategies in maintaining comfortable indoor conditions, this study introduces the Indoor Comfort Rate (ICR) concept. According to Eq. (9), a lower ICR reflects a more significant loss in thermal comfort, while a higher ICR signifies a better-maintained indoor thermal environment.

$$ICR = \left(\frac{\sum_{i=1}^{n} 1_{\{T_{in,i} \in [22,26]\}}}{T_{total}} \right) \times 100\% \quad (9)$$

Where $\sum_{i=1}^{n} 1_{\{T_{in,i} \in [T_{22,26}]\}}$ is the time that the indoor temperature is between 22 and 26 °C; T_{total} is the total monitoring time, h; n is the number of temperature records.

2.5.2. The physical comfort rate (PCR)

The floor surface temperature in heating systems significantly influences user comfort (mainly when walking barefoot), system efficiency, and long-term economic performance. As shown in Fig. 13, excessively high floor surface temperatures may cause discomfort or even burns, while overly low temperatures fail to provide adequate warmth, leaving occupants feeling cold. The optimal floor surface temperature depends on the specific usage scenario. The Chinese national design standard GB/T 50824-2013, Residential Building Energy Efficiency Design Standard, outlines the recommended average floor

Table 6
On-off control schedule for long-interval heating system.

Time	0h	6h	24h	30h	48h	54h	72h
Heating system	On	Off	On	Off	On	Off	Finish

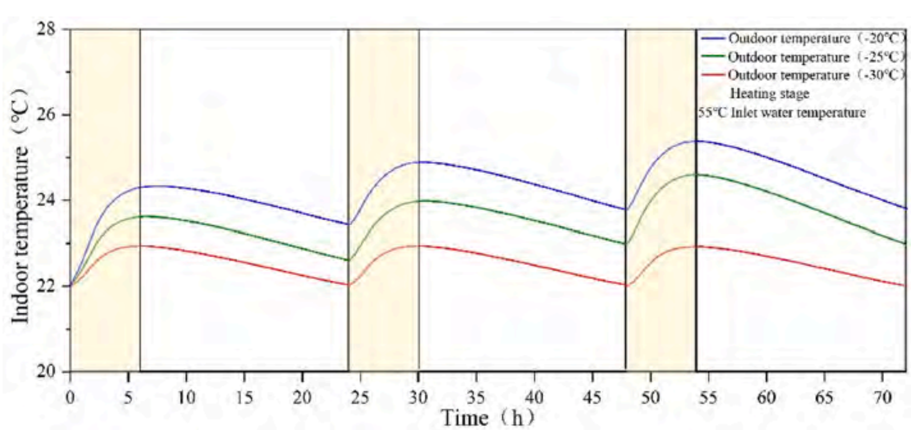

Fig. 11. Long-interval heating mode.

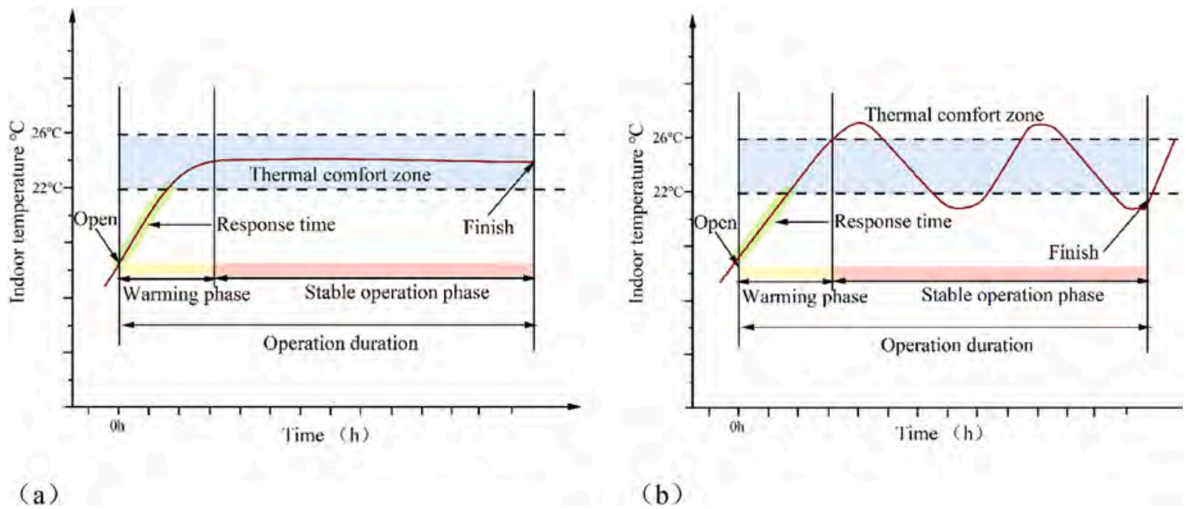

Fig. 12. Schematic diagram of indoor temperature changes: (a) Schematic diagram of indoor temperature changes in a residential building under continuous heating pattern, (b) Schematic diagram of indoor temperature changes in a residential building under intermittent heating pattern.

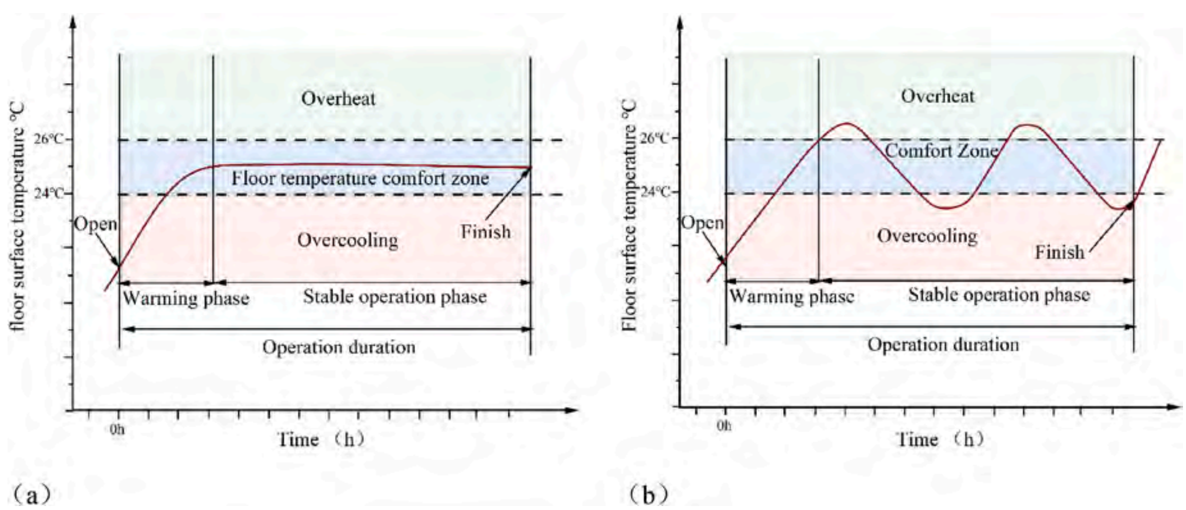

Fig. 13. Schematic diagram of floor surface temperature changes: (a) Schematic diagram of residential floor surface temperature changes under continuous heating; (b) Schematic diagram of residential floor surface temperature changes under intermittent heating.

surface temperature in Table 7 [85]. This study focuses on areas where people remain for extended periods, with the appropriate floor temperature range being 24 °C–26 °C.

To quantify the effectiveness of different heating strategies in maintaining actual human thermal comfort during heating, this study introduces the concept of the Physical Comfort Rate (PCR). PCR determines the percentage of time the floor surface temperature remains within the human comfort range during the heating system's operation. It can be calculated using Eq. (10). A higher PCR indicates that the heating strategy performed better at meeting actual human thermal comfort requirements.

Table 7
Average floor surface temperature requirements.

Environmental conditions	Suitable range(°C)	Maximum limit(°C)
Long-term occupancy areas	24–26	28
Short-term occupancy areas	28–30	32
Non-occupancy areas	35–40	42

$$PCR = \left(\frac{\sum_{i=1}^{n} 1_{\{T_{floor,i} \in [24,26]\}}}{T_{total}} \right) \times 100\% \tag{10}$$

Where $\sum_{i=1}^{n} 1_{\{T_{floor,i} \in [T_{24,26}]\}}$ is the time that floor surface temperature is between 24 and 26 °C; T_{total} is the total monitoring time, h; n is the number of temperature records.

2.5.3. Thermal response coefficient (TRC)

In addition, the Thermal Response Coefficient (TRC) reflects the speed at which the system affects indoor temperature when it is on, or its settings are adjusted. TRC is typically used to quantify the time required for a radiant floor heating system to reach the desired indoor temperature. By calculating the TRC, the performance of heating strategies can be better assessed. It can be determined using Eq. (11). A lower TRC indicates a faster system response, meaning the system can achieve the desired indoor temperature more quickly.

$$TRC = \frac{1}{T^{22^{\circ}C} - T^{open}} \tag{11}$$

where $T^{22^{\circ}C}$ is the time when the indoor temperature reaches 22 °C for the first time, h; T^{open} is the time when the heating system is turned on, h.

2.5.4. Energy consumption

Furthermore, the previously discussed evaluation metrics assess only the performance of heating strategies. To evaluate the energy efficiency of these strategies, this study uses energy consumption as a critical indicator. The energy consumption is calculated using Equations 12–14. A higher value of E_t indicates that the heating strategy consumes more energy.

$$E_t = MC\Delta t \tag{12}$$

$$M = V_t\rho \tag{13}$$

$$V_t = D_t v_t T_0 \tag{14}$$

Where M is mass; C is specific heat capacity; Δt is the temperature difference between inlet and outlet water; V_t is the volume of water; ρ is the density of water; D_t is the diameter of the floor heating pipe; v_t is the flow rate of the pipe diameter; T_0 is the operating time.

3. Results

3.1. Outdoor temperature

Fig. 14 depicts the indoor temperature variation of passive houses under the influence of different outdoor temperatures. Table 8 shows how outdoor temperature affects indoor temperature in passive houses.

As shown in Fig. 14(a)–(c) and (d)-(f), with consistent outdoor temperatures, the indoor temperature increases as the supply water temperature rises in both the continuous low-temperature heating mode and the long-interval heating mode. Fig. 14(g)–(i) illustrate that in the short-interval heating mode, the indoor temperature is less affected by the inlet water temperature, remaining stable between 22 °C and 26 °C. Additionally, Table 8 shows that for the same heating method under different outdoor temperatures, the maximum average temperature

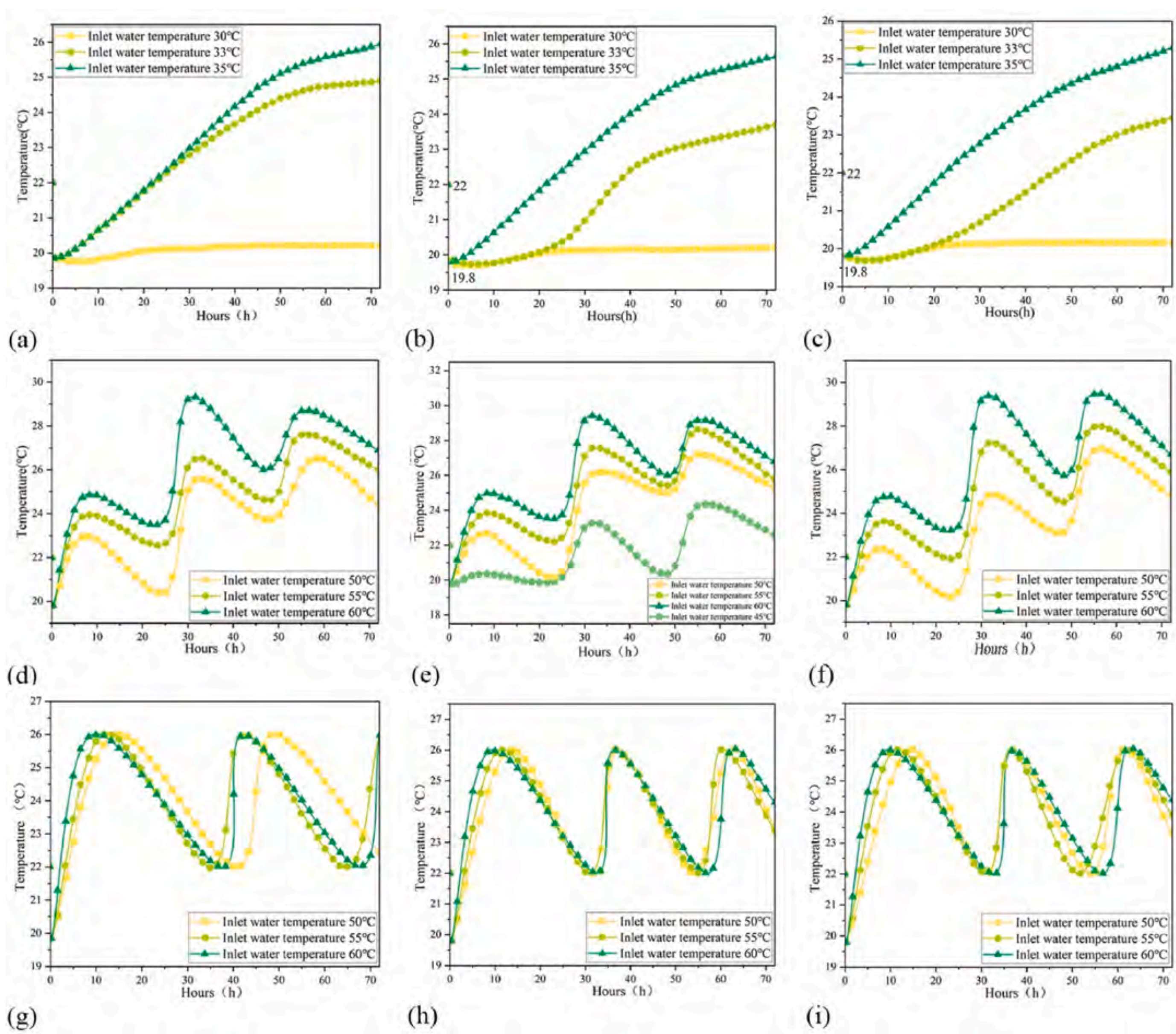

Fig. 14. Indoor temperature changes: (a)–(c) changes in indoor temperature under continuous low-temperature heating at outdoor temperatures of −20 °C, −25 °C, and −30 °C; (d)–(f) changes in indoor temperature under long-interval heating at outdoor temperatures of −20 °C, −25 °C, and −30 °C. (g)–(i) changes in indoor temperature under short-interval heating at outdoor temperatures of −20 °C, −25 °C, and −30 °C.

Table 8
Impact of outdoor temperature on indoor temperature.

Heating strategy	Continuous low temperature heating			Long-interval heating			Short-interval heating		
Inlet water temperature (°C)	30	33	35	50	55	60	50	55	60
Average temperature difference (°C)	0	0.5	0.3	0.5	0.5	0.3	0.2	0.5	0.4
Maximum temperature difference (°C)	0.05	0.9	0.65	1.4	1	0.8	0.8	2.08	1.7

difference is 0.5 °C, with a maximum temperature variation of 1.7 °C. The study results indicate that outdoor temperature minimally influences the selection of heating modes for passive houses. This is primarily due to the excellent insulation properties of passive houses, which significantly reduce heat loss and mitigate the impact of outdoor temperatures on indoor conditions. Therefore, user preferences primarily determine the choice of heating mode in passive houses. Based on this, the analysis in this paper uses simulation data at an outdoor temperature of −25 °C for further investigation.

3.2. Indoor comfort rate (ICR)

Fig. 15 illustrates indoor and pipe water temperature variation over time for the three heating strategies and ten heating methods applied in passive houses. For the continuous low-temperature heating strategy with inlet water temperatures of 30 °C, 33 °C, and 35 °C, the corresponding times to achieve thermal comfort were 0 h, 34 h, and 50.5 h, respectively. For the long-interval heating strategy with inlet water temperatures of 50 °C, 55 °C, and 60 °C, the times to reach thermal comfort were 34.5 h, 35 h, and 24.8 h, respectively. As shown in Fig. 15 (c), the overall average indoor temperature under the long-intermittent heating mode was relatively high; therefore, an additional simulation with an inlet water temperature of 45 °C was conducted, resulting in a thermal comfort time of 30 h. In contrast, for the short-interval heating strategy, with inlet water temperatures of 50 °C, 55 °C, and 60 °C, the corresponding thermal comfort times were 67.5 h, 68 h, and 68.3 h, respectively.

The Indoor Comfort Rate (ICR) for the ten heating methods is shown in Fig. 16. For the continuous low-temperature heating mode, the ICR values were 0 %, 47.2 % (50 %), and 70.1 % (70 %), respectively. In the long-interval heating mode, the ICR values were 41.6 % (40 %), 47.9 % (50 %), 70.1 % (70 %), and 34.4 % (30 %). For the short-interval heating mode, the effective indoor temperature guarantee rates were 93.8 % (90 %), 94.4 % (90 %), and 94.9 % (90 %), respectively. Therefore, the ICR for the short-interval heating mode remained above 90 %, outperforming both the continuous low-temperature heating mode and the long-interval heating mode. It can be seen that the short-interval heating strategies have certain advantages in ensuring indoor comfort.

3.3. The physical comfort rate (PCR)

Fig. 17shows the floor surface temperature variation over time for the three heating strategies. As shown in Fig. 17(a) and (b), the floor surface temperature increases with the rise in supply water temperature in both continuous low-temperature and long-interval heating modes. In the continuous low-temperature heating mode, the floor surface temperature remained within the optimal range for 0 h, 18 h, and 24.5 h, respectively. In the long-interval heating mode, the optimal floor surface temperature was maintained for 15.5 h, 23.5 h, 2.5 h, and 19 h, respectively. In contrast, the floor surface temperature remained within the optimal range for 67.5 h, 66.5 h, and 65 h for the short-interval heating mode.

Fig. 18 presents the Physical Comfort Rate (PCR) for the different heating strategies. The PCR for the continuous low-temperature heating mode was 0 %, 25 % (30 %), and 34 % (30 %), while for the long-interval heating mode, the PCR values were 21.5 % (20 %), 32.6 % (30 %), 3.5 % (0 %), and 26.3 % (30 %). For the short-interval heating mode, the PCR values were 93.8 % (90 %), 92.4 % (90 %), and 90.3 % (90 %). Therefore, the short-interval heating mode outperforms the continuous low-temperature and long-interval heating modes in terms of floor surface temperature comfort.

3.4. Thermal response coefficient (TRC)

Table 9 presents the thermal response times for the three heating control strategies in passive houses located in cold regions. Fig. 19 shows the Thermal Response Coefficients (TRC) for the different heating methods. For the continuous low-temperature heating mode, the TRC values were -, 0.026, and 0.047 h^{-1}. For the long-interval heating mode, the TRC values were 0.034, 0.222, 0.250, and 0.270 h^{-1}, while for the short-interval heating mode, the TRC values were 0.222, 0.250, and 0.270 h^{-1}. The TRC clearly relates to the supply water temperature—the higher the supply temperature, the higher the TRC. Therefore, the continuous low-temperature heating mode exhibited the least favorable TRC. However, an exception occurred in the long-interval heating mode with a 45 °C inlet water temperature, where the system had not yet reached the target indoor temperature of 22 °C before entering the second heating cycle, resulting in a longer thermal response time.

3.5. Energy consumption

Fig. 20 displays the operating time of the three heating strategies. Table 10 displays the energy consumption of the three heating strategies over a 72-h period.

For both the continuous low-temperature heating strategies and the long-interval heating strategies, energy consumption increases as the supply water temperature rises, given that the heating duration remains constant. The energy consumption for the three continuous low-temperature heating strategies is 36.43 kWh, 46.13 kWh, and 50.77 kWh, respectively. Similarly, the long-interval heating strategies consume 40.25 kWh, 55.21 kWh, 64.18 kWh, and 73.78 kWh of energy. In contrast, for the short-interval heating strategies, energy consumption decreases as the supply water temperature increases. The system's operating time reduces as the water temperature rises, partially offsetting the effect of the higher water temperature. As a result, the energy consumption for the three short-interval heating strategies remains relatively stable, at 63.95 kWh, 62.83 kWh, and 62.17 kWh, respectively. This demonstrates a strong correlation between the energy consumption of short-interval heating strategies and the building's airtightness and thermal insulation performance. The better the airtightness and insulation, the less energy is consumed.

In summary, while continuous low-temperature heating strategies may only achieve indoor thermal comfort slowly, they are more energy-efficient. Short-interval heating strategies have a manageable and relatively stable energy consumption, though slightly higher than continuous low-temperature strategies. However, because this study focuses on improving passive houses' indoor thermal environment, short-interval heating strategies are generally more effective than continuous low-temperature and long-interval heating strategies, making them more suitable for passive house use. For the case studied, the recommended indoor temperature control range is 22–26 °C, and a short-interval heating strategy with a water supply temperature of 60 °C can significantly enhance indoor thermal comfort.

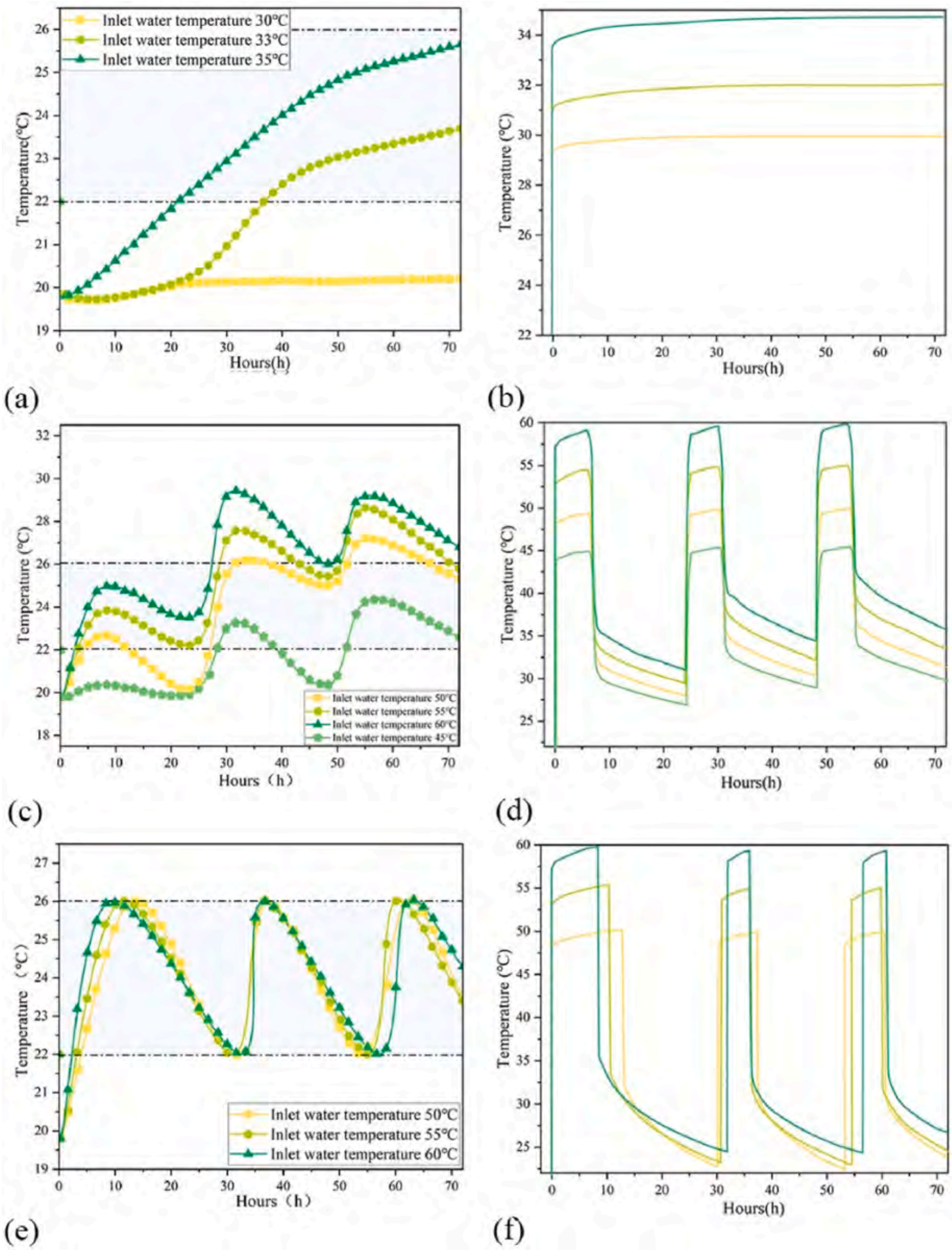

Fig. 15. Changes in indoor temperature and pipe water temperature: (a) and (b) changes in indoor temperature and pipe water temperature under the continuous low-temperature heating strategies, (c) and (d) changes in indoor temperature and pipe water temperature under the long-interval heating strategies, (e) and (f) changes in indoor temperature and pipe water temperature under the short-interval heating strategies.

4. Discussions

This study compared and analyzed heating strategies for passive houses in cold regions, proposing a control strategy for floor radiant heating systems based on indoor air temperature. Short-interval heating strategies significantly enhance indoor thermal comfort compared to continuous low-temperature and long-interval heating strategies. The analysis considered not only energy consumption but also the indoor comfort rate (ICR), physical comfort rate (PCR), and thermal response coefficient (TRC) to evaluate the heating strategies from an engineering perspective. Compared to traditional evaluation methods like the PMV-PPD index [45–47,86,90], this approach offers a more comprehensive

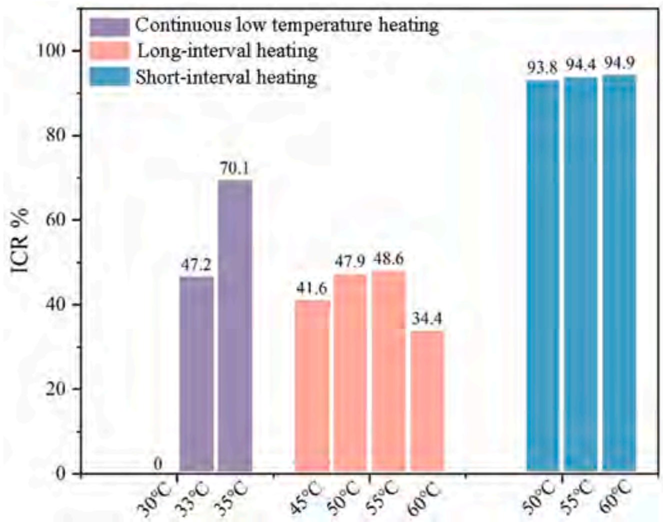

Fig. 16. The indoor comfort rate (ICR).

and intuitive assessment of heating performance.

The study simulated ten heating methods across three heating strategies at outdoor temperatures of −20 °C, −25 °C, and −30 °C. The results showed that the maximum average temperature difference for the same heating method was only 0.5 °C. While previous studies on traditional houses examined the influence of outdoor temperature on heating strategies [25,36,48], research on passive house heating strategies did not address this factor [21,22]. Comparative analysis revealed that passive houses have excellent thermal insulation, which significantly reduces heat loss and limits the effect of outdoor temperature on indoor conditions. Consequently, the simulation revealed that user needs, rather than the outdoor temperature, primarily determine heating strategy selection for passive houses, offering a novel direction for future research on passive house heating. Additionally, the study found that applying indoor air temperature-based heating strategies to radiant floor heating systems in passive houses is both feasible and effective, as shown by their superior performance compared to air conditioning systems [12,13,25]. For buildings with excellent airtightness, short-interval heating strategies are highly customizable and controllable, making them suitable for passive house heating.

Furthermore, in contrast to previous studies [37,38], this research used ICR, PCR, TRC, and energy consumption metrics to evaluate the three heating strategies comprehensively. Continuous low-temperature heating strategies had significantly lower ICR, PCR, and TRC values than short-interval strategies, although their energy consumption was also considerably lower. This suggests that short-interval heating strategies are more suitable for buildings requiring long-term heating with a focus on energy efficiency. In contrast, the long-interval heating strategy caused significant indoor temperature fluctuations, making it challenging to control ICR, PCR, and energy consumption. Thus, long-interval strategies are better suited for buildings with precise control needs (such as those with variable electricity pricing) and high thermal response coefficient requirements.

Based on indoor temperature control, the short-interval heating strategy resulted in ICR and PCR values above 90 % and a TRC above 0.2 h^{-1}, demonstrating its ability to respond quickly to indoor temperature changes while maintaining a thermally comfortable environment. Although its energy consumption was about 1.4 times higher than the continuous low-temperature heating strategy, it significantly improved indoor thermal comfort, meeting passive house heating needs. Therefore, adopting a short-interval heating strategy with an inlet water temperature of 60 °C and an indoor temperature range of 22 °C–26 °C is recommended to improve indoor comfort in passive houses.

5. Conclusion

This study aimed to provide efficient heating solutions for passive houses in cold regions by comparing three heating strategies' characteristics. It also examined the potential causes of differences in these

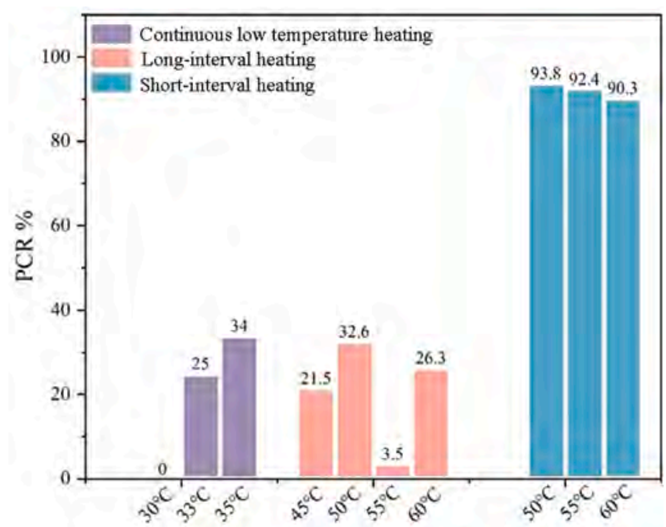

Fig. 18. The physical comfort rate (PCR).

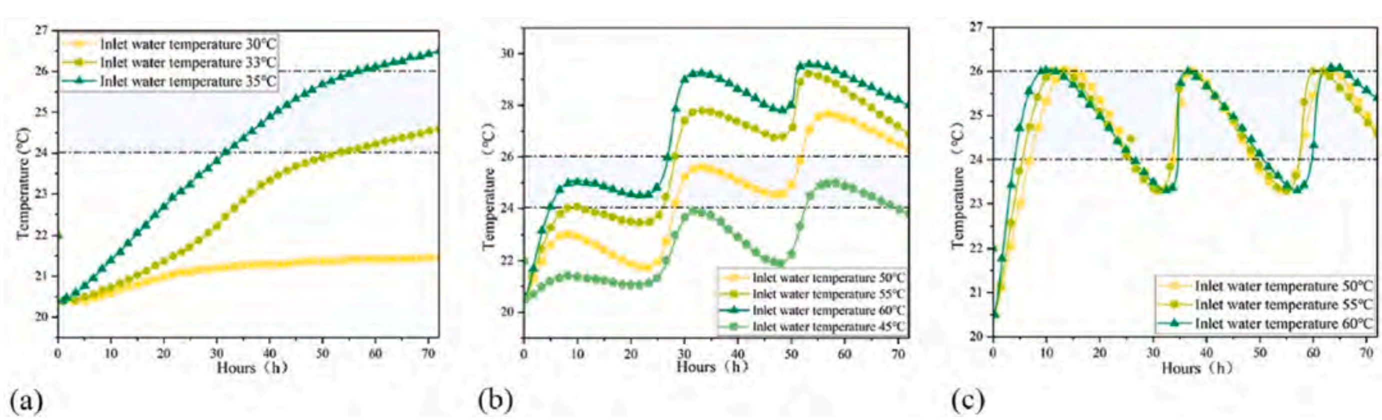

Fig. 17. Changes in floor surface temperature: (a) is the change in floor surface temperature under the continuous low-temperature heating strategies, (b) is the change in floor surface temperature under the long-interval heating strategies, and (c) is the change in floor surface temperature under the short-interval heating strategies.

Table 9
Response time.

Heating strategy	Continuous low temperature heating			Long-interval heating				Short-interval heating		
Water supply temperature	30 °C	33 °C	35 °C	45 °C	50 °C	55 °C	60 °C	50 °C	55 °C	60 °C
Thermal response (h)	–	38.0	21.5	29.0	4.5	4.0	3.7	4.5	4.0	3.7

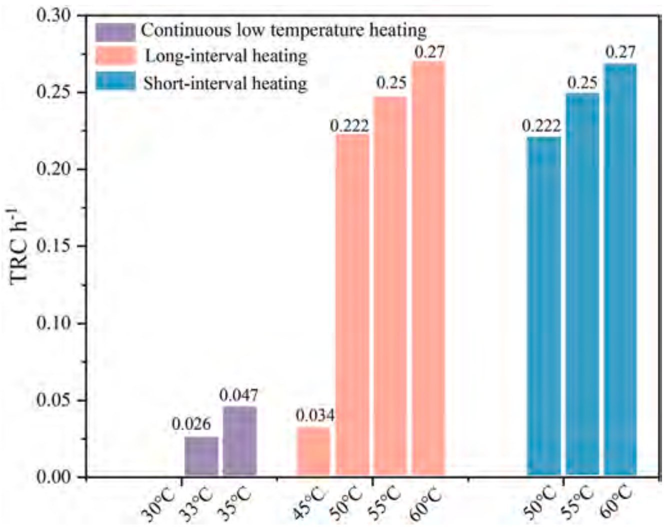

Fig. 19. Thermal response coefficient.

strategies, offering insights into more precise heating demand modeling in the future. The findings provide valuable references for selecting appropriate heating strategies for passive houses, as well as practical applications for improving indoor comfort. The main conclusions are as follows:

The impact of outdoor temperature fluctuation on the choice of heating strategies for passive houses is minimal. This study modeled nine heating methods across three heating strategies under three outdoor temperature conditions and compared the results to ensure rigorous simulation. The findings indicate that indoor users primarily influence the choice of heating strategy for passive house needs rather than outdoor temperature fluctuation. The continuous low-temperature heating strategy is suitable for buildings with long-term heating needs and a focus on minimizing energy consumption. This strategy has a higher Thermal Response Coefficient (TRC) because the inlet water temperature is lower. This implies that selecting the appropriate inlet water temperature is crucial to ensure that the Indoor Comfort Rate (ICR) and Physical Comfort Rate (PCR) satisfy user requirements in a thermally stable state.

For buildings with specific control requirements (e.g., peak-valley electricity pricing) and a high demand for a low TRC, the long-interval heating strategy is appropriate. However, controlling this strategy is more challenging, as it depends on operating time and inlet water temperature. Testing the optimal operating mode is necessary to ensure that the ICR and PCR meet user expectations. The short-interval heating strategy is ideal for spaces where high ICR, PCR, and TRC are required, but energy consumption is less of a concern. The energy consumption of this strategy closely correlates with the building's airtightness and insulation, providing high controllability. As a result, the short-interval heating strategy is a great choice for buildings with excellent airtightness and insulation performance.

Based on these findings, this study recommends adopting the short-interval heating mode for passive houses, with an inlet water temperature of 60 °C and an indoor temperature control range of 22–26 °C. This strategy achieves ICR and PCR values above 90 %, as well as a TRC above 0.2 h^{-1}. Although its energy consumption is 1.4 times that of the continuous low-temperature heating strategy, the fluctuating outdoor temperatures in cold regions, which do not consistently fall below −20 °C for long periods, result in shorter heating durations. Thus, the short-interval heating strategy is recommended in passive houses, where high ICR, PCR, and TRC are prioritized over energy consumption.

In this research, three types of floor radiant heating systems in passive houses in severely cold regions are simulated and analyzed, considering the effects of outdoor and inlet water temperatures.

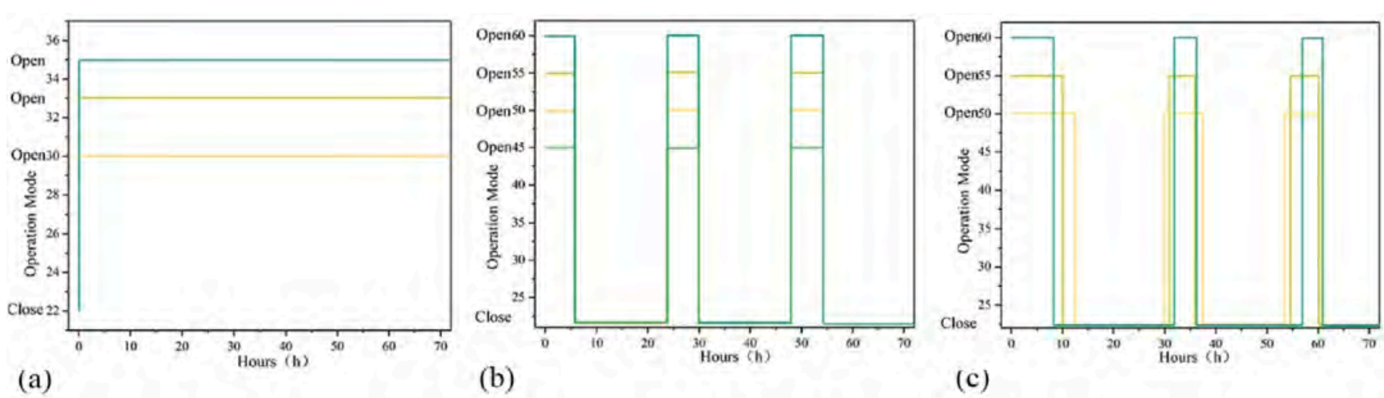

Fig. 20. Operating time: (a) is the operating time of continuous low-temperature heating, (b) is the operating time of long-interval heating, and (c) is the operating time of short-interval heating.

Table 10
Energy consumption of different heating strategies.

Heating strategy	Continuous low temperature heating			Long-interval heating				Short-interval heating		
Water supply temperature	30 °C	33 °C	35 °C	45 °C	50 °C	55 °C	60 °C	50 °C	55 °C	60 °C
Energy consumption (kWh)	36.43	46.13	50.77	40.28	55.21	64.18	73.78	63.95	62.83	62.17

However, several limitations remain. The study did not examine the impact of factors such as the number of occupants or furniture on the heating strategies of passive houses. Moreover, the effects of occupant movement and window ventilation on the indoor thermal environment were not considered. Furthermore, with respect to the heat source, the research mainly focuses on heating strategies under extreme cold conditions (−20 °C, −25 °C, −30 °C) and briefly describes the application of high-efficiency air source heat pumps, solar thermal systems, energy storage systems, and auxiliary electric heating systems. However, the comprehensive coordination among different heat sources and their specific impacts on heating performance have not been explored in depth. Therefore, as passive house technology evolves, future research could further investigate the optimization of heating strategies in complex dynamic environments. Moreover, the synergistic effects of various heat source combinations under extreme climatic conditions should be explored, alongside an investigation of how smart control systems can optimize heat source distribution to improve system energy efficiency and occupant comfort.

CRediT authorship contribution statement

Xiaoni Gao: Writing – review & editing, Writing – original draft, Visualization, Validation, Software, Methodology, Investigation. **Yuchen Ji:** Validation, Investigation, Data curation. **Pengyuan Shen:** Writing – review & editing, Writing – original draft, Supervision, Methodology, Funding acquisition, Formal analysis, Conceptualization.

Declaration of competing interest

The authors declare that they have no known competing financial interests or personal relationships that could have appeared to influence the work reported in this paper.

Data availability

Data will be made available on request.

References

[1] Xu S, Wang Y, Niu J, Ma G. 'Coal-to-electricity'project is ongoing in north China. Energy 2020;191:116525.
[2] Shen P, Wang Z, Ji Y. Exploring potential for residential energy saving in New York using developed lightweight prototypical building models based on survey data in the past decades. Sustain Cities Soc 2021;66:102659.
[3] Shen P. Building energy retrofit optimization considering future climate and decision-making under various mindsets. J Build Eng 2024:110422.
[4] Georges L, Berner M, Mathisen HM. Air heating of passive houses in cold climates: investigation using detailed dynamic simulations. Build Environ 2014;74:1–12.
[5] Welch S, Obonyo E, Memari A. A review of the previous and current challenges of passive house retrofits. Build Environ 2023:110938.
[6] Jayasena A, Hewage K, Siddiqui O, Sadiq R. Socio-economic and environmental cost-benefit analysis of passive houses: a life cycle perspective. J Clean Prod 2022;373:133718.
[7] Ridley I, Clarke A, Bere J, Altamirano H, Lewis S, Durdev M, et al. The monitored performance of the first new London dwelling certified to the Passive House standard. Energy Build 2013;63:67–78.
[8] Cho J, Park B, Lim T. Experimental and numerical study on the application of low-temperature radiant floor heating system with capillary tube: thermal performance analysis. Appl Therm Eng 2019;163:114360.
[9] Wang Y, Kuckelkorn J, Zhao F-Y, Spliethoff H, Lang W. A state of art of review on interactions between energy performance and indoor environment quality in Passive House buildings. Renew Sustain Energy Rev 2017;72:1303–19.
[10] Shen P, Braham W, Yi Y. The feasibility and importance of considering climate change impacts in building retrofit analysis. Appl Energy 2019;233–234:254–70.
[11] Guo Z, Zhang W, Deng G, et al. The impact of window opening behavior on the indoor thermal environment and coping strategies in passive houses. Energy Built Environ 2024. https://doi.org/10.1016/j.enbenv.2024.04.003.
[12] Stephan A, Crawford RH, De Myttenaere K. A comprehensive assessment of the life cycle energy demand of passive houses. Appl Energy 2013;112:23–34.
[13] Mihai M, Tanasiev V, Dinca C, Badea A, Vidu R. Passive house analysis in terms of energy performance. Energy Build 2017;144:74–86.
[14] Colclough S, Salaris C. Quantifying overheating in nZEB Irish residential buildings. An analysis of recorded interior temperatures of Irish newbuild and retrofit residential buildings against CIBSE, Passive House and WHO overheating criteria and recorded occupant satisfaction. Energy Build 2024;303:113571.
[15] Liu Y, Yu Z, Song C, Wang D. Heating load reduction characteristics of passive solar buildings in Tibet, China. Conference Heating load reduction characteristics of passive solar buildings in Tibet, China. Springer, p. 1-20.
[16] Xifeng Z, Shu-wen N, Guang-hua L, Li-na Y. The heating effect of the additional solar house to classroom in the cold region—A case study of an elementary school. Energy Proc 2012;14:1193–8.
[17] Wei L, Dan L, Baiyi L, Min Z. Effect analysis of a passive solar house in Tibet. Aasri Procedia 2012;3:619–23.
[18] Zhang L, Hou Y, Du J, Xu L, Zhang G, Shi L. Trombe wall for a residential building in Sichuan-Tibet alpine valley–A case study. Renew Energy 2020;156:31–46.
[19] Qi D, Liu Y, Zhao C, Dong Y, Song B, Li A. Thermal response and performance evaluation of floor radiant heating system based on fuzzy logic control. Energy Build 2024:114232.
[20] Hooshmand SM, Zhang H, Javidanfar H, Zhai Y, Wagner A. A review of local radiant heating systems and their effects on thermal comfort and sensation. Energy Build 2023:113331.
[21] Kong X, Chang Y, Fan M, Li H. Analysis on the thermal performance of low-temperature radiant floor coupled with intermittent stratum ventilation (LTR-ISV) for space heating. Energy Build 2023;278:112623.
[22] Benakopoulos T, Vergo W, Tunzi M, Salenbien R, Kolarik J, Svendsen S. Energy and cost savings with continuous low temperature heating versus intermittent heating of an office building with district heating. Energy 2022;252:124071.
[23] Rhee K-N, Kim KW. A 50 year review of basic and applied research in radiant heating and cooling systems for the built environment. Build Environ 2015;91:166–90.
[24] Ali AHH, Gaber Morsy M. Energy efficiency and indoor thermal perception: a comparative study between radiant panel and portable convective heaters. Energy Effic. 2010;3:283–301.
[25] Wang Z, Wang F, Ma Z, Bai M, Liu S. Experimental investigation and evaluation of the performance of air-source heat pumps for indoor thermal comfort control. J Mech Sci Technol 2018;32:1437–47.
[26] Badran AA, Jaradat AW, Bahbouh MN. Comparative study of continuous versus intermittent heating for local residential building: case studies in Jordan. Energy Convers Manag 2013;65:709–14.
[27] Meng X, Huang Y, Cao Y, Gao Y, Hou C, Zhang L, et al. Optimization of the wall thermal insulation characteristics based on the intermittent heating operation. Case Stud Constr Mater 2018;9:e00188.
[28] Li Y, Long E, Zhang L, Dong X, Wang S. Energy-saving potential of intermittent heating system: influence of composite phase change wall and optimization strategy. Energy Explor Exploit 2021;39(1):426–43.
[29] Xu B, Zhou S, Hu W. An intermittent heating strategy by predicting warm-up time for office buildings in Beijing. Energy Build 2017;155:35–42.
[30] Lu L, Wen J, Chen J, Liu X. Study on material parameter optimization for improving the heat transfer performance of lightweight floor radiant heating. J Build Eng 2024:108698.
[31] Lund H, Duic N, Østergaard PA, Mathiesen BV. Future district heating systems and technologies: on the role of smart energy systems and 4th generation district heating. Energy 2018;165:614–9.
[32] Neirotti F, Noussan M, Riverso S, Manganini G. Analysis of different strategies for lowering the operation temperature in existing district heating networks. Energies 2019;12(2):321.
[33] Sun C, Yan H, Cao S, Xia G, Liu Y, Wu X. A control strategy considering buildings' thermal characteristics to mitigate heat supply-demand mismatches in district heating systems. Energy 2024:132637.
[34] Liu Y, Nan X, Han H, Li J. The variable water temperature control strategy of the air-source heat pump compatible with floor heating system for an apartment. J Build Eng 2024;90:109440.
[35] Mao N, Hao J, He T, Song M, Xu Y, Deng S. PMV-based dynamic optimization of energy consumption for a residential task/ambient air conditioning system in different climate zones. Renew Energy 2019;142:41–54.
[36] Dong Z, Boyi Q, Pengfei L, Zhoujian A. Comprehensive evaluation and optimization of rural space heating modes in cold areas based on PMV-PPD. Energy Build 2021;246:111120.
[37] Xu Z, Liu F, Xu W, Wang Z, Yang Y, Xu C, et al. Atmospheric air quality in Beijing improved by application of air source heat pump (ASHP) systems. J Clean Prod 2020;257:120582.
[38] Ma S, Liu W, Dong J, Liu J, Wang Z. Indoor thermal environment in a rural dwelling heated by air-source heat pump air-conditioner. Sustain Energy Technol Assessments 2022;51:101948.
[39] Zhang S, Cheng Y, Fang Z, Lin Z. Dynamic control of room air temperature for stratum ventilation based on heat removal efficiency: method and experimental validations. Build Environ 2018;140:107–18.
[40] Zampetti L, Arnesano M, Revel G. Experimental testing of a system for the energy-efficient sub-zonal heating management in indoor environments based on PMV. Energy Build 2018;166:229–38.
[41] Fang J, Feng Z, Cao S-J, Deng Y. The impact of ventilation parameters on thermal comfort and energy-efficient control of the ground-source heat pump system. Energy Build 2018;179:324–32.
[42] Mao N, Pan D, Li Z, Xu Y, Song M, Deng S. A numerical study on influences of building envelope heat gain on operating performances of a bed-based task/ambient air conditioning (TAC) system in energy saving and thermal comfort. Appl Energy 2017;192:213–21.

[43] Mao N, Pan D, Deng S, Chan M. Thermal, ventilation and energy saving performance evaluations of a ductless bed-based task/ambient air conditioning (TAC) system. Energy Build 2013;66:297–305.
[44] Mao N, Hao J, Cui B, Li Y, Song M, Xu Y, et al. Energy performance of a bedroom task/ambient air conditioning (TAC) system applied in different climate zones of China. Energy 2018;159:724–36.
[45] Song Z, Xia Y, Ma M, Deng B, Miao T, Fan Q, et al. Reliable sleep temperature regulation based on PMV model and dynamic thermal parameters. Build Environ 2024;254:111420.
[46] Custódio DA, Ghisi E, Rupp RF. Thermal comfort in university classrooms in humid subtropical climate: field study during all seasons. Build Environ 2024;258: 111644.
[47] Alfano FRdA, Ianniello E, Palella BI. PMV–PPD and acceptability in naturally ventilated schools. Build Environ 2013;67:129–37.
[48] Fanger PO. Thermal Comfort: Analysis and Applications in Environmental Engineering. Copenhagen, Denmark: Danish Technical Press; 1970. p. 75–150.
[49] Li K, Zheng W, Xue W, Wang Z. Fast reconstruction of indoor temperature field for large-space building based on limited sensors: an experimental study. Energy Build 2023;298:113493.
[50] Jia X, Cao B, Zhu Y, Huang Y. Field studies on thermal comfort of passengers in airport terminals and high-speed railway stations in summer. Build Environ 2021; 206:108319.
[51] Ali SF, Sharma L, Rakshit D, Bhattacharjee B. Influence of passive design parameters on thermal comfort of an office space in a building in Delhi. J Architect Eng 2020;26(3):04020017.
[52] Shen P, Wang M, Liu J, Ji Y. Hourly air temperature projection in future urban area by coupling climate change and urban heat island effect. Energy Build 2023;279: 112676.
[53] Wang M, Shen P. Investigation of indoor asymmetric thermal radiation in Tibet plateau: case study of a typical office building. Buildings 2022;12(2):129.
[54] Shen P, Liu J, Wang M. Fast generation of microclimate weather data for building simulation under heat island using map capturing and clustering technique. Sustain Cities Soc 2021;71:102954.
[55] Bae Y, Nam K, Kang S. CFD-ML: Stream-based active learning of computational fluid dynamics simulations for efficient product design. Comput Ind 2024;161: 104122.
[56] Li J, Ma R, Deng M, Cao X, Wang X, Wang X. A comparative study of clustering algorithms for intermittent heating demand considering time series. Appl Energy 2024;353:122046.
[57] Qu M, Sang X, Yan X, Huang P, Zhang B, Bai X. A simulation study on the heating characteristics of residential buildings using intermittent heating in Hot-Summer/ Cold-Winter areas of China. Appl Therm Eng 2024;241:122360.
[58] Chen X, Li Z, Dai L, Zeng W, Liu Z, Liu M. Characteristics of intermittent heating by air source heat pump in rural areas of northern China based on indoor temperature effective guarantee rate. J Build Eng 2024;95:110196.
[59] Wang Y, Dong Q, Guo H, Yin L, Gao W, Yao W, et al. Indoor thermal comfort evaluation of traditional dwellings in cold region of China: a case study in Guangfu Ancient City. Energy Build 2023;288:113028.
[60] Wang H, Wang S. A hierarchical optimal control strategy for continuous demand response of building HVAC systems to provide frequency regulation service to smart power grids. Energy 2021;230:120741.
[61] Qin M, Chew BT, Yau YH, Han X, Yang Z, Cui T, et al. A novel evaluation indicator and optimal heating strategy for using an intermittent-operation catalytic combustion heater in open cold environments. Build Environ 2024;252:111271.
[62] Ruiz GR, Bandera CF. Analysis of uncertainty indices used for building envelope calibration. Appl Energy 2017;185:82–94.
[63] Ramos Ruiz G, Fernandez Bandera C. Validation of calibrated energy models: common errors. Energies 2017;10(10):1587.
[64] Pachano JE, Bandera CF. Multi-step building energy model calibration process based on measured data. Energy Build 2021;252:111380.
[65] Možina M, Pajek L, Nadarajah PD, Singh MK, Košir M. Defining the calibration process for building thermal performance simulation during the warm season: a case study of a single-family log house. Adv Build Energy Res 2024:1–36.
[66] Blight TS, Coley DA. Sensitivity analysis of the effect of occupant behaviour on the energy consumption of passive house dwellings. Energy Build 2013;66:183–92.
[67] Qu M, Yan X, Sang X, Bai Y, Chu W, Zhu X. Field studies on indoor thermal environment and start-stop characteristics of the radiant air conditioning system during intermittent heating. J Build Eng 2023;76:107121.
[68] Pan Y-H, Zhao R, Fan X-H, Nian Y-L, Cheng W-L. Study on the effect of varying channel aspect ratio on heat transfer performance of manifold microchannel heat sink. Int J Heat Mass Tran 2020;163:120461.
[69] Charvátová H, Zálešák M, Sehnálek S. Parameterization of module for testing of thermal stability in the room. Latest Trends on Systems.2:647-650.
[70] Pryor RW. Multiphysics modeling using COMSOL 5 and MATLAB: mercury learning and information. 2021.
[71] Al Musleh M, Topriska EV, Jenkins D, Owens E. Thermoelectric generator characterization at extra-low-temperature difference for building applications in extreme hot climates: experimental and numerical study. Energy Build 2020;225: 110285.
[72] Pryor RW. Multiphysics modeling using COMSOL®: a first principles approach. Jones & Bartlett Publishers; 2009.
[73] Charvátová H, Procházka A, Zálešák M. Computer simulation of temperature distribution during cooling of the thermally insulated room. Energies 2018;11(11): 3205.
[74] Wang J, Shan X, Hu P, Zhang C, Yuan D, Hu X, et al. Bioinspired multilayer structures for energy-free passive heating and thermal regulation in cold environments. ACS Appl Mater Interfaces 2022;14(41):46569–80.
[75] Chen X, Xue P, Liu L, Gao L, Liu J. Outdoor thermal comfort and adaptation in severe cold area: a longitudinal survey in Harbin, China. Build Environ 2018;143: 548–60.
[76] Leng H, Chen X, Ma Y, Wong NH, Ming T. Urban morphology and building heating energy consumption: evidence from Harbin, a severe cold region city. Energy Build 2020;224:110143.
[77] Li C, Zhou D, Wang H, Cheng H, Li D. Feasibility assessment of a hybrid PV/diesel/ battery power system for a housing estate in the severe cold zone—a case study of Harbin, China. Energy 2019;185:671–81.
[78] Wang Z, Zhang L, Zhao J, He Y, Li A. Thermal responses to different residential environments in Harbin. Build Environ 2011;46(11):2170–8.
[79] Mlakar J, Štrancar J. Overheating in residential passive house: solution strategies revealed and confirmed through data analysis and simulations. Energy Build 2011; 43(6):1443–51.
[80] Berge M, Mathisen HM. The suitability of air-heating in residential passive house buildings from the occupants' point of view–a review. Adv Build Energy Res 2015; 9(2):175–89.
[81] Xue Q, Wang Z. Investigation and simulation on indoor thermal environment of a passive residential building in severe cold area of China. Procedia Eng 2017;205: 3578–84.
[82] Wang Z, Xue Q, Ji Y, Yu Z. Indoor environment quality in a low-energy residential building in winter in Harbin. Build Environ 2018;135:194–201.
[83] Jaouaf S, Bensaad B, Habib M. Passive strategies for energy-efficient educational facilities: insights from a mediterranean primary school. Energy Rep 2024;11: 3653–83.
[84] Tan X, Wang Y, Wu L, Yu Y, Yu Q, Sun G. An ANFIS-Based indirect control strategy for solar heating system: exploring PMV approach. Energy Build 2024;309:114056.
[85] Sun C, Yuan L, Chen Y, Cao S, Xia G, Qi C, et al. An intelligent control and regulation strategy aiming at building level heating balance in district heating system. Energy 2023;278:127941.
[86] Li Z, Wei W, Wang W, Sun Y, Wang S, Lin Y, et al. A method for sizing air source heat pump considering the joint effect of outdoor air temperature and relative humidity. J Build Eng 2023;65:105815.
[87] Djamila H. Indoor thermal comfort predictions: selected issues and trends. Renew Sustain Energy Rev 2017;74:569–80.
[88] Fan G, Xie J, Yoshino H, Yanagi U, Hasegawa K, Wang C, et al. Investigation of indoor thermal environment in the homes with elderly people during heating season in Beijing, China. Build Environ 2017;126:288–303.
[89] Junghans L, Widerin P. Thermal comfort and indoor air quality of the "Concept 22/ 26". a new high performance building standard. Energy and Buildings 2017;149: 114–22.
[90] Li Q, Zhang L, Zhang L, Wu X. Optimizing energy efficiency and thermal comfort in building green retrofit. Energy 2021;237:121509.